Discovery of Novel Small Molecule Inhibitors of Dengue Viral NS2B-NS3 Protease Using Virtual Screening and Scaffold Hopping

Jing Deng,[†,⊥] Ning Li,[‡,⊥] Hongchuan Liu,[‡,⊥] Zhili Zuo,[§,⊥] Oi Wah Liew,[‖] Weijun Xu,[§] Gang Chen,[§] Xiankun Tong,[‡] Wei Tang,*[,‡] Jin Zhu,[†] Jianping Zuo,[‡] Hualiang Jiang,[†,‡] Cai-Guang Yang,*[,‡] Jian Li,*[,†] and Weiliang Zhu*[,‡]

[†]Shanghai Key Laboratory of New Drug Design, School of Pharmacy, East China University of Science and Technology, 130 Mei Long Road, Shanghai 200237, China

[‡]Shanghai Institute of Materia Medica, Chinese Academy of Sciences, 555 Zu Chong Zhi Road, Shanghai 201203, China

[§]Centre for Biomedical and Life Sciences, Singapore Polytechnic, 500 Dover Road, Singapore 139651

[‖]Cardiovascular Research Institute, Yong Loo Lin School of Medicine, National University of Singapore, 14 Medical Drive, Singapore 117599

ⓈSupporting Information
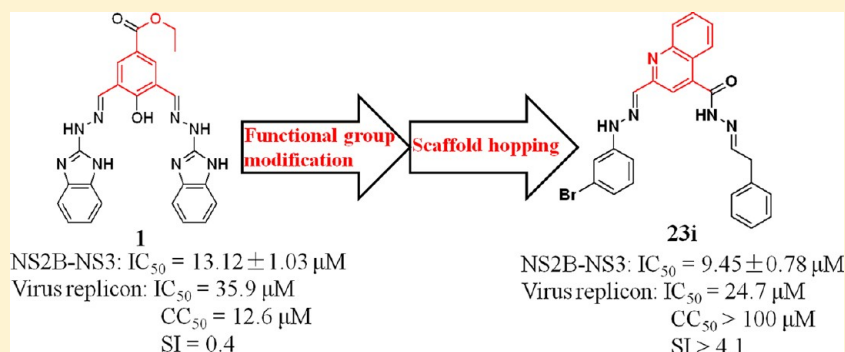
ABSTRACT: By virtual screening, compound **1** was found to be active against NS2B-NS3 protease (IC$_{50}$ = 13.12 ± 1.03 μM). Fourteen derivatives (**22**) of compound **1** were synthesized, leading to the discovery of four new inhibitors with biological activity. In order to expand the chemical diversity of the inhibitors, small-molecule-based scaffold hopping was performed on the basis of the common scaffold of compounds **1** and **22**. Twenty-one new compounds (**23**, **24**) containing quinoline (new scaffold) were designed and synthesized. Protease inhibition assays revealed that 12 compounds with the new scaffold are inhibitors of NS2B-NS3 protease. Taken together, 17 new compounds were discovered as NS2B-NS3 protease inhibitors with IC$_{50}$ values of 7.46 ± 1.15 to 48.59 ± 3.46 μM, and 8 compounds belonging to two different scaffolds are active to some extent against DENV based on luciferase reporter replicon-based assays. These novel chemical entities could serve as lead structures for discovering therapies against DENV.

1. INTRODUCTION

Dengue viruses (DENVs), transmitted by *Aedes aegypti* mosquitoes, belong to the *Flavivirus* genus that includes other serious pathogens such as tick-borne encephalitis viruses, West Nile viruses (WNVs), yellow fever viruses (YFVs), and Japanese encephalitis viruses (JEVs).[1] There are four serotypes of dengue (DENV 1−4), each of which can cause dengue disease. The infection severity ranges from the mild dengue fever (DF) to the more serious dengue hemorrhagic fever (DHF) and dengue shock syndrome (DSS).[2] The World Health Organization has estimated that the dengue viruses infect 50−100 million people each year and threaten up to 2.5 billion people in more than 100 countries, especially in the tropical and subtropical regions.[3−5] Approximately 500 000 infected people develop DHF and DSS, leading to 22 000 deaths, and the infection numbers have been on the rise

globally in recent years.[6] Currently there is no approved vaccine or a targeted drug therapy available for treatment of dengue infection.[7] Accordingly, development of a safe, effective therapeutic agent for dengue viruses is urgently needed.

DENV is an enveloped RNA virus with ~11 kb positive-strand RNA genome, which is transcribed and translated into a single polypeptide upon entering the host cell.[8] Subsequently, the single polypeptide is processed by host cell proteases and the virus-encoded NS2B-NS3 protease to generate three structural proteins (capsid protein, precursor-membrane protein, and envelope protein) and seven nonstructural proteins (NS1, NS2A, NS2B, NS3, NS4A, NS4B, and NS5).[9] The 184-residue NS3pro, with multiple enzyme activities that

are required for viral replication, is a trypsin-like protease with a serine protease catalytic triad (His51, Asp75, and Ser135).[10,11] The proteolytic activity of NS3pro can be markedly enhanced when it is coupled to its cofactor, the central hydrophilic portion (residues 49−95) of NS2B.[12,13] Optimal catalytic activity of NS3 depends on the presence of NS2B.[14] The NS2B-NS3 protease mediated post-translational proteolytic processing of the viral polyprotein is essential for the maturation and pathogenesis of dengue virus.[15,16] Consequently, NS2B-NS3 protease is considered as a promising target for antidengue virus drug development.

A number of different strategies have been employed to search for DENV NS2B-NS3 protease inhibitors,[17,18] including synthesizing rationally designed substrate-based peptidomimetics[19−21] or cyclopeptide[22] and structure-based virtual screening,[23−25] as well as screening natural products[26−28] and small compound libraries.[29] However, only a few peptide or small molecule inhibitors of the DENV NS2B-NS3 protease with moderate activity have so far been reported.[17,18] Although several peptide or cyclopeptide inhibitors against DENV NS2B-NS3 protease have been reported with IC_{50} values lower than submicromolar range,[19−21] the undesirable physicochemical features and high toxicity may limit their further development. Lam and co-workers[22] have prepared some kalata B1 analogues and revealed that two oxidized forms of cyclopeptide could be substrate-competitive inhibitors of the dengue viral NS2B-NS3 protease with K_i of 1.39 ± 0.35 and 3.03 ± 0.75 μM, respectively. Watowich et al.[23,24] reported two compounds with inhibitory activity against the DENV protease in vitro and antiviral activity against DENV-2 in cell culture (EC_{50} of 4.2 ± 1.9 and 35 ± 8 μM). After further studies, they improved the inhibitory activities of anthracene-based compounds ranging between ∼2- and 60-fold (with K_i decreased). Just recently, a small molecule inhibitor BP2109 with moderate enzymatic activity against DENV NS2B-NS3 protease (IC_{50} = 15.43 ± 2.12 μM) was reported to show more potency in the dengue virus replicon-based assay (EC_{50} = 0.17 ± 0.01 μM).[29] Other known compounds[23−25,30] also need further optimization to be therapeutically useful, as they either have limited potency or are not druglike compounds.

Toward this end, we initiated a program aimed at seeking novel small molecule inhibitors of dengue viral NS2B-NS3 protease. A schematic representation of the discovery process of the inhibitors is shown in Figure 1. Briefly, by use of a

Figure 1. Schematic representation of the inhibitors' discovery strategy adopted.

docking-based virtual screening on ∼600 000 compounds in the ACD database, 27 predicted hits were bought and tested for NS2B-NS3 protease inhibitory activity, leading to the discovery of three active small molecule compounds (**1**−**3**) with different scaffolds (Figure 2). Compound **1** was selected as the starting point for further structural optimization in considering inhibitory activity, structural variability, and synthetic accessibility. Then functional group modification and scaffold hopping approaches were used in turn for structural optimization of compound **1**. In total, 35 new analogues (**22a**−**n**, **23a**−**m**, and **24a**−**h**, Figure 3) have been designed, synthesized, and tested. Taken together, in this study 17 compounds (**1**, **22a**, **22j**, **22l,m**, **23a**−**e**, **23g**−**j**, **23l**, and **24g,h**) were discovered to show moderate dengue viral NS2B-NS3 protease inhibition in vitro, and eight compounds (**1**, **22j**, **23b**, **23i,j**, **23l**, and **24g,h**) are active to some extent against the replication of the dengue viral replicon in vitro. These compounds could be used as leads for further search for small molecule dengue viral NS2B-NS3 protease inhibitors with better potency.

2. METHODS

2.1. Computation. *2.1.1. Structure Based Virtual Screening.* Here we used the highest quality structure of unliganded DEN NS3pro-NS2B (PDB code 2FOM)[31] with resolution of 1.5 Å for virtual screening. The structure represents the virtually active protease, as NS2B has a pronounced effect on both stability and the catalytic activity of NS3pro (3300- to 6600-fold).[13] This structure was actually used in our previous study for molecular docking.[14] About 600 000 compounds in the chemical database ACD (available chemical database, http://www.mdli.com/products/experiment/available_chem_dir/index.jsp) were prepared for virtual screening. Two molecular docking programs DOCK 4.0[32,33] and GOLD 3.0[34] are quite suitable for the system according to our previous VS protocol and result.[14] All water molecules were removed from the NS3pro-Ns2B structures. Hydrogen atoms were added, and Amber95 atomic charges were assigned to all protein atoms using standard Sybyl, version 6.8,[35] protocols. To estimate the binding strength between ligands and target protein, a three-dimensional grid of 0.3 Å resolution centered on a proper protein pocket, which is near the catalytic site,[14] was generated with CHEMGRID using an all atom model, where a $1/(4r)$ distance-dependent dielectric factor and a 10 Å distance cutoff were set for nonbonded interactions. Residues around Leu149 at a radius of 10 Å were isolated for the construction of the grid for docking simulation. This radius was large enough to include all residues that were involved in putative inhibitor binding site. On average, 100 orientations were sampled for each small molecule. The bump filter was used with bump maximum of 3. In addition, all ligand configurations were subjected to maximum 50 steps of simplex rigid body minimization (convergence of 0.1 Å). The distance filter was used in the matching calculation. Neither chemical labeling nor critical points were used in the docking calculation. No decoy database was used for validating the VS protocol, as few that are potent could be found during the early stage of this study.

2.1.2. Small Molecule Based Scaffold Hopping. Functional group modifications on R_1−R_4 substituents in compound **1** (Figure 3) resulted in four new inhibitors with moderate inhibition activity in vitro. We switched to perform structural optimization that mainly focused on the core structure replacement (scaffold hopping)[36] in compound **1** (red part, Figure 3). Given the docked binding pose of compound **1** in
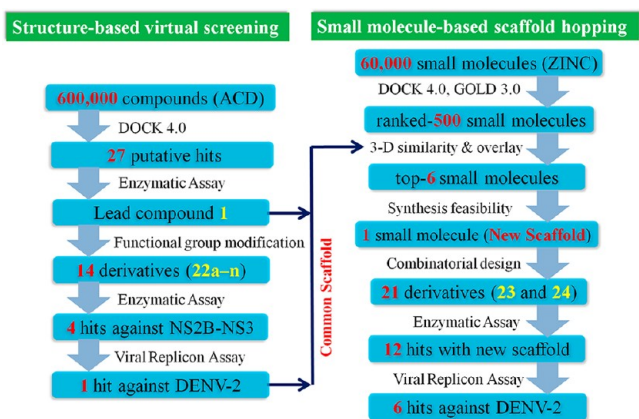
1 (IC$_{50}$ = 13.1 μM)   **2** (IC$_{50}$ = 242.4 μM)   **3** (IC$_{50}$ = 219.9 μM)
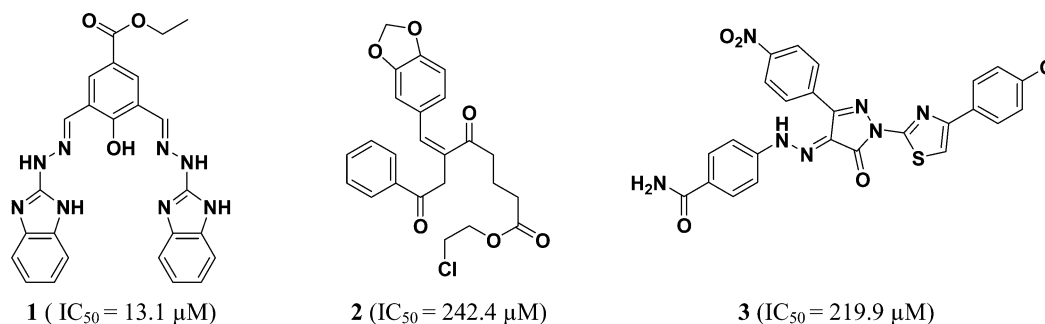
Figure 2. Structures of DENV NS2B-NS3 protease inhibitors **1**−**3** discovered by virtual screening and their inhibitory activities.
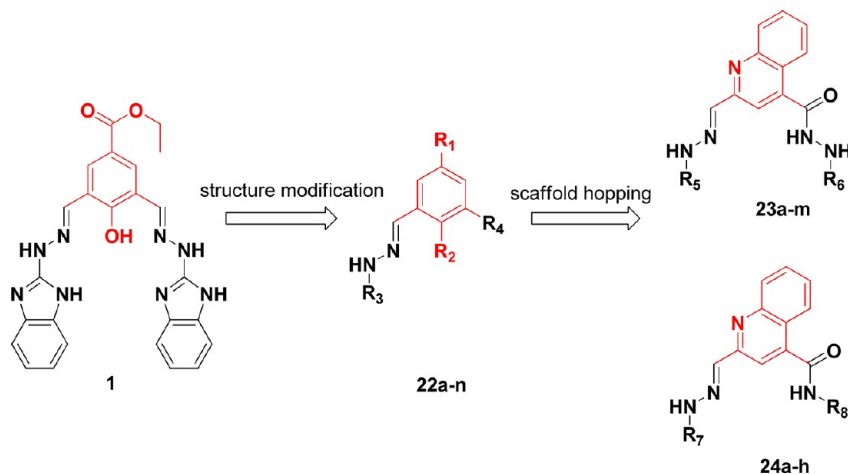
Figure 3. Evolution process from lead compound **1** to analogues **22**, **23**, and **24** is shown. The structures of R$_1$−R$_8$ are presented in Tables 1−3.
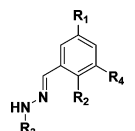
the binding pocket of NS2B-NS3 protease, the phenyl moiety (old scaffold) of compound **1** (middle, Figure 3) could be replaced by different small molecules (new scaffold). To quickly find a new scaffold, we prepared a small molecule data set containing approximately 60 000 small molecules from the ZINC library (xLogP ≤ 2.5; MW ≤ 250; the number of rotatable bonds of ≤5). The 3D structures of all the small molecules were generated by Concord Standalone with the ionization state at pH 7, which were subsequently optimized using the Powell method with Tripos force field and Gasteiger−Marsilli charges in Sybyl.[35] The same parameter settings were used in the docking step as those for virtual screening. The small molecule data set was screened, and the top 6000 small molecules generated from the energy scoring function of DOCK 4.0[32,33] were then reevaluated by GOLD 3.0[34] (genetic optimization for ligand docking). The top 500 molecules from GOLD 3.0 were selected for similarity and synthetic feasibility analysis. The default parameters in GOLD 3.0 were used except that a maximum number of 300 000 operations and a population of 200 individuals were imposed. The most reasonable binding poses of different small molecules in the pocket of NS3-NS2B were identified by the sequential evaluation of GoldScore and ChemScore fitness function, which then were used for overlay with the binding pose of compound **1**. After visual inspection of the docked compounds in the binding site, the fragments fitting nicely with the phenyl moiety of compound **1** were selected as potential new moieties for scaffold-hopping (red part, Figure 3). The whole process was called scaffold hopping using 3D overlay in the binding site. All the virtual screening and small-molecule-based scaffold
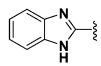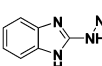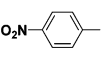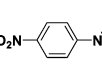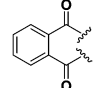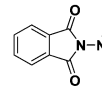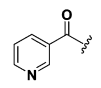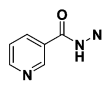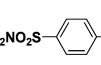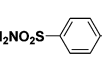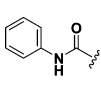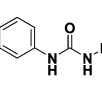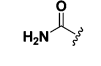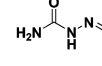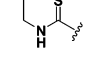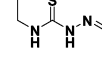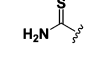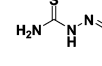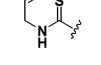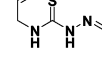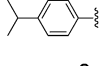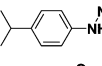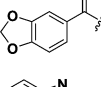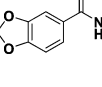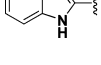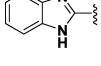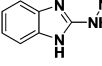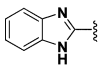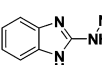
hopping were performed on SGI Origin3800 computer at the Shanghai Institute of Materia Medica.

2.2. Chemistry. *2.2.1. Design of Analogues of Compound 1.* Compound **1** (Figure 2) was obtained from the ACD database by virtual screening. To provide expedient and significant structure−activity relationship (SAR) information and improve the inhibitory activity of lead compound **1**, chemical modifications were performed in two cycles (Figure 3). In the first round, we incorporated various steric, electronic, and hydrophobic groups at substituted positions 3 and 5 on the benzene ring (R$_3$ and R$_4$, Figure 3) in compound **1**; thus, 11 analogues (**22a**−**k**) were designed and prepared (Table 1). To test if the double hydrazone substituents phenolic hydroxy (R$_2$, Figure 3) and carbethoxy (R$_1$, Figure 3) on the benzene ring are necessary for ligand−enzyme interaction, we designed and synthesized three more analogues (compounds **22l**−**n**, Table 1). In the second round, to further improve inhibitory activity and expand chemical diversity, we discovered two new series of compounds **23** and **24** (Figure 3) through small-molecule-based scaffold hopping. In total, 21 compounds (**23a**−**m** and **24a**−**h**), containing a quinoline moiety (new scaffold) and different side chain substituents, were synthesized to explore their inhibitory activity on NS2B-NS3 protease (Tables 2 and 3).

2.2.2. Synthetic Procedures. Scheme 1 depicts the synthetic route for the preparation of compound **1** and its derivatives **22a**−**l**. Esterification of 4-hydroxy-3,5-dimethylbenzoic acid **4** in reflux ethanol easily afforded ethyl 4-hydroxy-3,5-dimethylbenzoate **5**, followed by acetylation with acetic anhydride to give ethyl 4-acetoxy-3,5-dimethylbenzoate **6** in good yield. Oxidation of this intermediate with chromium trioxide/sulfuric

Table 1. Chemical Structures of Compounds 1 and 22a−n and Their Activities

Entry	cmpd	R_1	R_2	R_3	R_4	$IC_{50}{}^a$ (μM) (inhibitory rate at 100 μM)
1	1	-CO₂Et	-OH			13.12±1.03
2	22a	-CO₂Et	-OH			14.58±2.06
3	22b	-CO₂Et	-OH			>100 (27.98%)
4	22c	-CO₂Et	-OH			NA
5	22d	-CO₂Et	-OH			NA
6	22e	-CO₂Et	-OH			>100 (44.11%)
7	22f	-CO₂Et	-OH			NA
8	22g	-CO₂Et	-OH			>100 (28.2%)
9	22h	-CO₂Et	-OH			>100 (24.42%)
10	22i	-CO₂Et	-OH			NA
11	22j	-CO₂Et	-OH			39.46±1.43
12	22k	-CO₂Et	-OH			>100 (35.44%)
13	22l	-CO₂Et	-OH		-Me	48.59±3.46
14	22m	-CO₂Et	-H			29.53±2.15
15	22n	-H	-OH			>100 (31.90%)

^{a}Data are the mean values of three independent experiments.
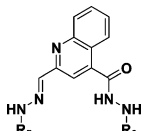
acid in a mix solvent of acetic anhydride and acetic acid at 0 °C afforded compounds **7a** and **7b**, respectively. Target hydrazones **1** and **22a−l** were synthesized by reacting **7a** and **7b** with hydrazines, hydrazides, aminoguanidines, or semicarbazides. Compounds **22m−n** were prepared from **8** and **11** similarly (Schemes 2 and 3).

Compounds **23a−m** were synthesized through the approach outlined in Scheme 4. Treatment of isatin **14** with acetone in potassium hydroxide solution under reflux afforded 2-methylquinoline-4-carboxylic acid **15**, followed by esterification

with ethanol to yield ethyl 2-methylquinoline-4-carboxylate **16**. Oxidation of this intermediate with selenium dioxide in dioxane solution under reflux afforded compound **17** in high yield. Then compound **17** was substituted by different phenylhydrazines, giving **18**, which was converted to the corresponding hydrazide **19** by refluxing with hydrazine hydrate. Reaction of **19** with different aldehydes in ethanol afforded compounds **23a−m**.

Compounds **24a−h** were synthesized through the route shown in Scheme 5. 2-Formylquinoline-4-carboxylic acid **20**

Table 2. Chemical Structures of Compounds 23a–m and Their Activities

Entry	cmpd	R₅	R₆	IC₅₀[a] (μM) (inhibitory rate at 100 μM)
1	23a	2-Cl-phenyl	phenylpropyl	29.04±1.78
2	23b	2-Cl-phenyl	styryl	28.12±1.96
3	23c	3-Cl-phenyl	cinnamyl	14.32±2.49
4	23d	4-sulfonamide-phenyl	3-OH-styryl	7.83±0.94
5	23e	4-sulfonamide-phenyl	phenylpropyl	36.02±3.05
6	23f	4-sulfonamide-phenyl	styryl	>100 (31.06%)
7	23g	4-sulfonamide-phenyl	cinnamyl	7.46±1.15
8	23h	3-Br-phenyl	phenylpropyl	19.93±0.98
9	23i	3-Br-phenyl	styryl	9.45±0.78
10	23j	3-NO₂-phenyl	cinnamyl	21.96±2.05
11	23k	3-CF₃-phenyl	phenylpropyl	>100 (20.95%)
12	23l	3-CF₃-phenyl	styryl	19.8±1.15
13	23m	3-CF₃-phenyl	cinnamyl	>100 (27.44%)

[a]Data are the mean values of three independent experiments.

Table 3. Chemical Structures of Compounds 24a–h and Their Activities

Entry	cmpd	R₇	R₈	IC₅₀[a] (μM) (inhibitory rate at 100 μM)
1	24a	4-sulfonamide-phenyl	phenylpropyl	>100 (20.61%)
2	24b	4-sulfonamide-phenyl	phenylbutyl	>100 (29.35%)
3	24c	3-Br-phenyl	phenylpropyl	>100 (24.17%)
4	24d	3-Br-phenyl	phenylbutyl	>100 (30.64%)
5	24e	3-Cl-phenyl	phenylpropyl	>100 (32.15%)
6	24f	3-Cl-phenyl	phenylbutyl	NA
7	24g	2-COOH-phenyl	phenylpropyl	41.24±5.53
8	24h	2-COOH-phenyl	phenylbutyl	35.28±4.36

[a]Data are the mean values of three independent experiments.

was prepared by the oxidation of compound **15** with selenium dioxide in dioxane solution. Amidation of compound **20** with 3-phenylpropan-1-amine or 4-phenylbutan-1-amine mediated by 1-ethyl-3-(3′-dimethylaminopropyl)carbodiimide (EDCI) readily provided the desired compounds **21**. Target hydrazones **24a–h** were synthesized by reacting compounds **21** with different phenylhydrazines.

2.3. Biological Assays. *2.3.1. In Vitro Protease Inhibition Assays.* The hydrophilic core sequence of the NS2B cofactor (residues 49–95) linked to the NS3 protease domain (residues 1–184) via a flexible glycine linker (GGGGSGGGG) was used for expression of NS2B-NS3 protease.[37] The purification of NS2B-NS3 protease was performed as described in a known procedure.[38] For protease inhibition assays, the small molecule inhibitors in 10 concentrations (ranging from 0.8 to 400 μM) were mixed with DENV-2 NS2B-NS3pro (final concentration at 100 nM) in the assay buffer (50 mM Tris-HCL, 1 mM CHAPS, 20% glycerol, pH 9.0) and then preincubated at 25 °C

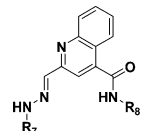for 15 min. Inhibitor solutions were prepared from stock in DMSO (final DMSO concentration in the assay was less than 1%). Then catalysis was initiated by adding substrate (Dabcyl-Lys-Gln-Arg-Arg-Gly-Arg-Ile-Glu-Edans, purchased from Shanghai GL Biochem Ltd. and directly used without further purification) to a final concentration of 10 μM. The fluorescence increase was continuously monitored every 2 min for 30 min at room temperature using Flex Station 3 (Molecular Devices), and the excitation wavelength of 340 nm and the emission wavelength of 450 nm were used. IC₅₀ values were determined from plots of percent activity over compound concentration using sigmoidal dose−response by GraphPad Prism software (San Diego, CA, U.S.). Triplicate measurements were taken for each data point. All data are reported as the mean ± SE.

2.3.2. In Vitro Antiviral Assays. 2.3.2.1. Dengue Virus Replicon. A DENV-2 replicon carrying a firefly luciferase gene as reporter was constructed using an infectious full length DENV2 plasmid pD2FT, which was derived from the DENV2 (New Guinea C strain) cDNA. Initially, the structure protein coding sequence of CprME was deleted by PCR method. The Luc-IRES-APH gene cassette was constructed in a pMD18 vector. Then the PCR amplified gene cassette was ligated with pD2FT which, lacking most of the structure gene coding sequence, resulted in a DENV2 replicon plasmid driven by a T7 protomer named pD2RepT. Replicon genome diagram is shown in Figure 4. The plasmid was linearized by XbaI and replicon RNA was transcribed using the Ribomax T7 RNA synthesis kit (Promega) in the presence of cap analogue m7GpppA (NEB). Replicon RNA was then transfected into BHK cell using Lipofectamin 2000 reagent. Cells were cultured

Scheme 1[a]
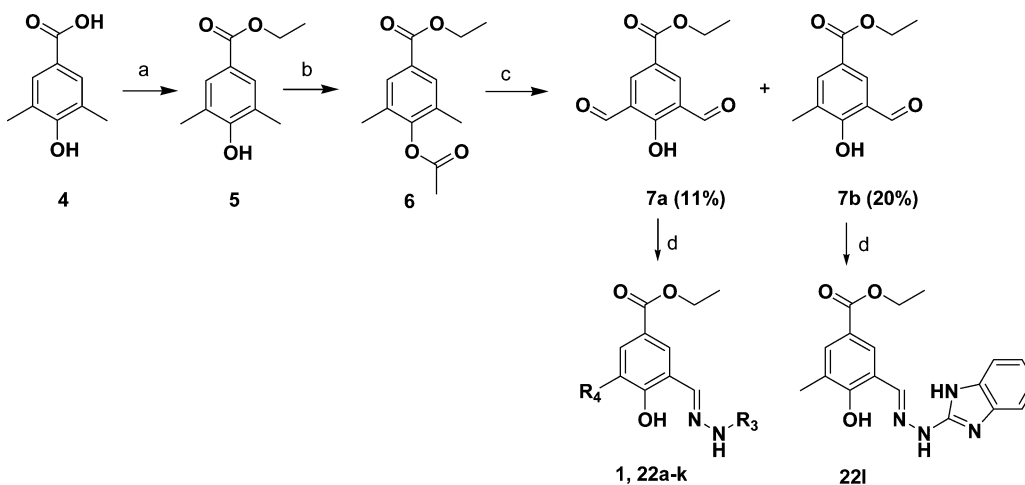
[a]Reagents and conditions: (a) conc H$_2$SO$_4$, EtOH, reflux, 15 h; (b) Ac$_2$O, reflux, overnight; (c) (i) CrO$_3$, Ac$_2$O, conc H$_2$SO$_4$, AcOH, 0 °C, 20 h; (ii) conc H$_2$SO$_4$, EtOH, reflux, 1 h; (d) AcOH, EtOH, 80 °C, 2 h.

Scheme 2[a]
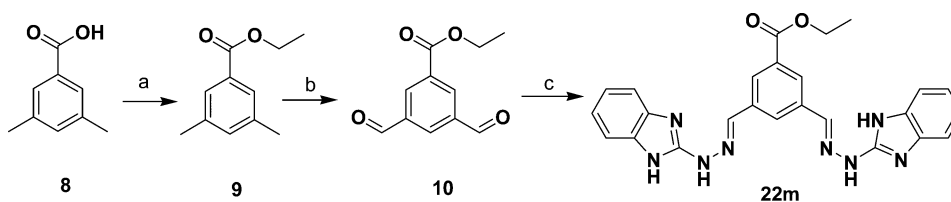
[a]Reagents and conditions: (a) conc H$_2$SO$_4$, EtOH, reflux, 15 h; (b) (i) CrO$_3$, Ac$_2$O, conc H$_2$SO$_4$, AcOH, 0 °C, 20 h; (ii) conc H$_2$SO$_4$, EtOH, reflux, 1 h; (c) AcOH, EtOH, 80 °C, 2 h.

Scheme 3[a]
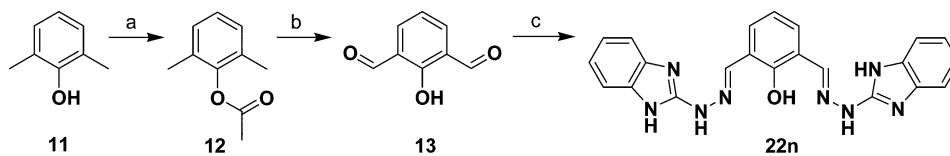
[a]Reagents and conditions: (a) Ac$_2$O, reflux, overnight; (b) (i) CrO$_3$, Ac$_2$O, conc H$_2$SO$_4$, AcOH, 0 °C, 20 h; (ii) conc H$_2$SO$_4$, EtOH, reflux, 1 h; (c) AcOH, EtOH, 80 °C, 2 h.

Scheme 4[a]
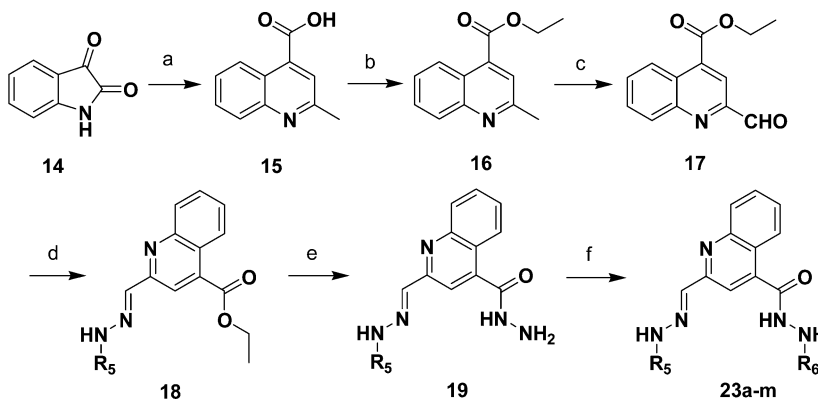
[a]Reagents and conditions: (a) (i) acetone, aq KOH, reflux, 15 h; (ii) conc HCl; (b) conc H$_2$SO$_4$, EtOH, reflux, 18 h; (c) SeO$_2$, dioxane, reflux, 4 h; (d) AcOH, EtOH, 80 °C, 2 h; (e) N$_2$H$_4$·H$_2$O, 120 °C, 20 h; (f) AcOH, EtOH, 80 °C, 2 h.

in DMEM medium containing 10% FBS and 400 μg/mL G418 (Invitrogen). Resistant clones expressing the highest amount of luciferase and viral nonstructural proteins were selected and used as a DENV2 replicon cell line named BHK-D2RepT

Scheme 5[a]
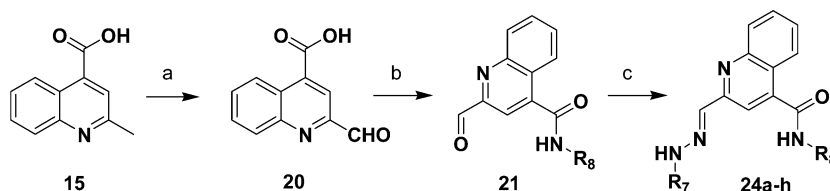
[a]Reagents and conditions: (a) SeO$_2$, dioxane, reflux, 4 h; (b) EDCI, HOBt, TEA, CH$_2$Cl$_2$, rt, overnight; (c) AcOH, EtOH, 80 °C, 2 h.

Figure 4. Schematic diagram of the DENV-2 reporter replicon (DV2Rep).
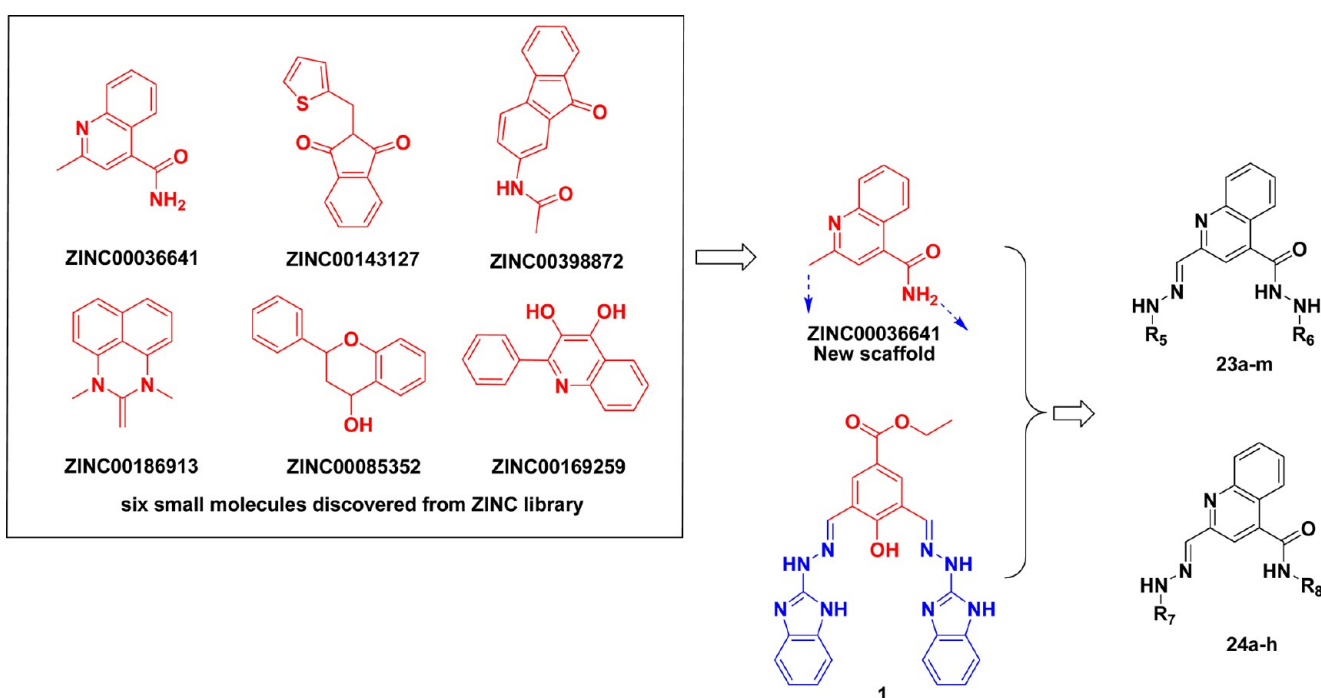
Figure 5. Compound **1** directed scaffold hopping based on the six small molecules (new scaffold) selected from the ZINC library.

(Figure 4). Cells were propagated in DMEM medium containing 10% FBS and 200 µg/mL G418.

2.3.2.2. Inhibition of the Replication of the Dengue Virus Replicon. BHK-D2RepT cells were seeded in white 96-well plates (Costar) at densities of 5× 10^4 cells per well for 24 h. Compounds were dissolved in DMSO as stocking solution, then diluted to appropriate concentration using medium and added into cell culture medium. Final concentration of DMSO in the culture medium was less than 0.2% (v/v). Cells were then cultured for another 48 h in the presence of compounds. Before luciferase readout, culture medium was replaced with DMEM medium and luciferase signal was assayed by Bright-Glo firefly luciferase assay kit (Promega). In each 96-well plate, incubations were done in triplicate and six control wells were also included. The inhibitory rate was calculated as the percentage of luciferase signals compared with control wells without compound. Experiments carried out in the 96-well plate format, with BHK cells or BHK-D2RepT-replicon containing cells, allowed us to calculate IC$_{50}$ (the inhibitory

concentration that led to 50% of the control luciferase signals) and CC$_{50}$ (the concentration that led to 50% of the control cell number) of selected compounds.

2.3.3. Cytotoxicity Assays. Besides the above-mentioned antiviral assays, an MTT [3-(4,5-dimethylthiazol-2-yl)-2,5-diphenyltetrazolium bromide] assay was performed to estimate compound cytotoxicity. Approximately 5 × 10^4 BHK cells (nontransfected cells) per well were seeded to a 96-well plate. On the following day, the cells were incubated with various concentrations of the compound for 48 h. Cell viability was then quantified using an MTT assay.

3. RESULTS AND DISCUSSION

3.1. Identification of Compound 1 by Virtual Screening. Targeting the crystal structure of DENV NS2B-NS3 complex, we screened ~600 000 compounds in the ACD database by molecular docking. On the basis of the docking score and binding modes, we purchased 27 samples for activity test. Finally, compounds **1–3** were found to be active against
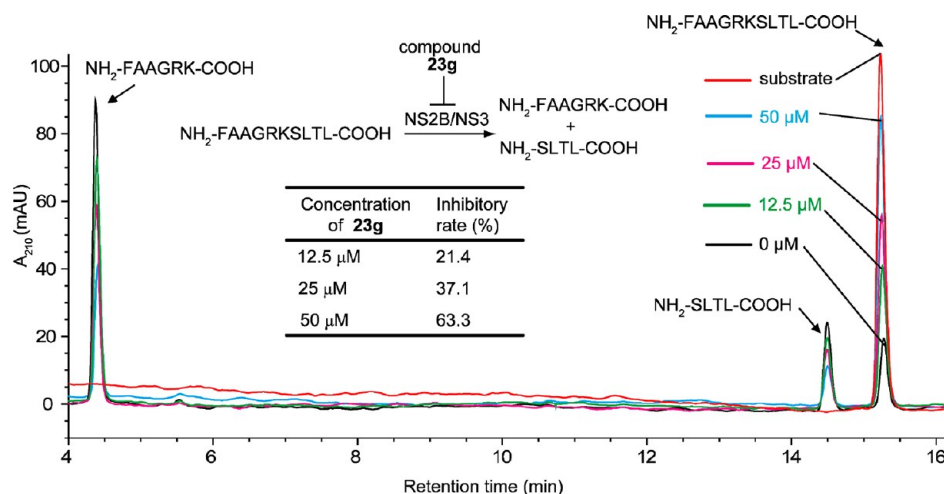
Figure 6. Compound **23g** dose-dependently inhibited DENV-2 NS2B-NS3 protease in the cleavage of substrate peptide NH$_2$-FAAGRKSLTL-COOH by reversed-phase HPLC. HPLC traces showed the substrate peptide (red) and the inhibition of cleavage of substrate peptide by 1 μM protease in the presence of inhibitor **23g** at 0 μM (black), 12.5 μM (green), 25 μM (magenta), and 50 μM (cyan).

DENV-2 NS2B-NS3 protease with IC$_{50}$ of 13.1−242.4 μM. Compound **1** was then identified as lead structure for further optimization after considering the biological activity, structural variability, and synthetic accessibility.

3.2. Discovery of New Scaffold by Scaffold Hopping. We initially used the DOCK 4.0 program to screen a small molecule database of the ZINC library containing about 60 000 small molecules (xLogP ≤ 2.5; MW ≤ 250; the number of rotatable bonds of ≤5). The top 6000 hits were then evaluated by GoldScore fitness function and ChemScore fitness function sequentially, and the best-fitting binding modes of ranked 500 small molecules were selected for conformational comparison with the phenyl moiety of compound **1** (red part, Figure 3). By overlay with the binding pose of compound **1** in the pocket of NS2B-NS3, 6 small molecules out of the top 500 compounds with higher 3D similarity to the phenyl moiety of compound **1** were chosen after visual inspection. Among them, ZINC00036641 has been proved to possess reliable synthetic feasibility by querying the Beilstein database (CrossFire Beilstein) and its quinoline moiety could be used for replacement of the phenyl moiety of compound **1** (Figure 5). On this basis, we continued to design a variety of derivatives by combining the core moiety of ZINC00036641 with various substitutions of compound **1**, leading to compounds **23a−m** and **24a−h**.

3.3. Analogue Design and Synthesis. In total, 36 compounds (**1**, **22a−n**, **23a−m**, and **24a−h**) were designed and synthesized, and their chemical structures are shown in Tables 1−3. These compounds were synthesized through the routes outlined in Schemes 1−5, and the details for synthetic procedures and structural characterizations are described in the Experimental Section. All of the compounds are dissolvable in dimethylsulfoxide (DMSO) and methanol (MeOH) with high lipophilicity. All compounds (**1**, **22a−n**, **23a−m**, and **24a−h**) were confirmed to have 95% purity (Supporting Information Table 1S).

3.4. Biological Activities. *3.4.1. In Vitro Protease Activity Inhibition.* For DENV-2 NS2B-NS3 protease activity assays, an internally quenched fluorescent peptide substrate Dabcyl-KQRRGRIE-Edans was designed and commercially synthesized. The K_m of our purified DENV NS2B-NS3 protease on Dabcyl-KQRRGRIE-Edans was determined to be 16.31 ± 4.15

μM. For the primary assay, the percent inhibition against DENV NS2B-NS3 protease of the tested compounds at 100 μM was measured. All compounds with hydrazone fluorescence would appear as false positives in the protease assay, so the testing condition we used was carefully optimized for minimizing the potential interference using the same compound and peptide substrate without protease as reference. Next, to rule out the false-positive inhibitory activities of our compounds, we performed a reversed-phase HPLC-based assay[39] that is orthogonal to the fluorescence-based assay. We used the most potent compound **23g** as an example to test its inhibitory activity against NS2B-NS3 protease (for the materials and methods of this assay, see Supporting Information). As shown in Figure 6, compound **23g** was inhibitory active in a dose-dependent manner with 63.3%, 37.1%, and 21.4% of inhibition rate at 50, 25, and 12.5 μM, respectively, based on the decrease of peak area of peptide substrate in the HPLC trace. These inhibition data are consistent with the results observed in the fluorescence-based inhibition assay, which proves that the fluorescence-based protease inhibition assays employed in this study are reliable.

Then the compounds with inhibitory rates of more than 50% were used for further study to determine their half-maximal inhibitory concentration (IC$_{50}$) against DENV NS2B-NS3 protease. A typical inhibitory progress curve of compound **1** in different concentrations is shown in Figure 7A. Figure 7B shows that compound **1** dose-dependently inhibited DENV NS2B-NS3 protease in the cleavage of substrate by IC$_{50}$ of 13.12 ± 1.03 μM. These results indicated that compound **1** was a good candidate inhibitor worthy of structure modification and optimization.

In the first round of structure modification, we tested the DENV NS2N-NS3 protease activities of compound **1** and its derivatives **22a−n**. The results are summarized in Table 1. Of the synthetic derivatives tested, only four derivatives (**22a**, **22j**, and **22l,m**) displayed moderate inhibitory activity (IC$_{50}$ ranging from 14.58 ± 2.06 to 48.59 ± 3.46 μM), less potent than compound **1** (IC$_{50}$ = 13.12 ± 1.03 μM). The results of the first cycle modification of compound **1** turned out to be unsatisfactory but still acceptable.

After we obtained compounds **23a−m** and **24a−h** through scaffold hopping, 12 new compounds (**23a−e**, **23g−j**, **23l**, and
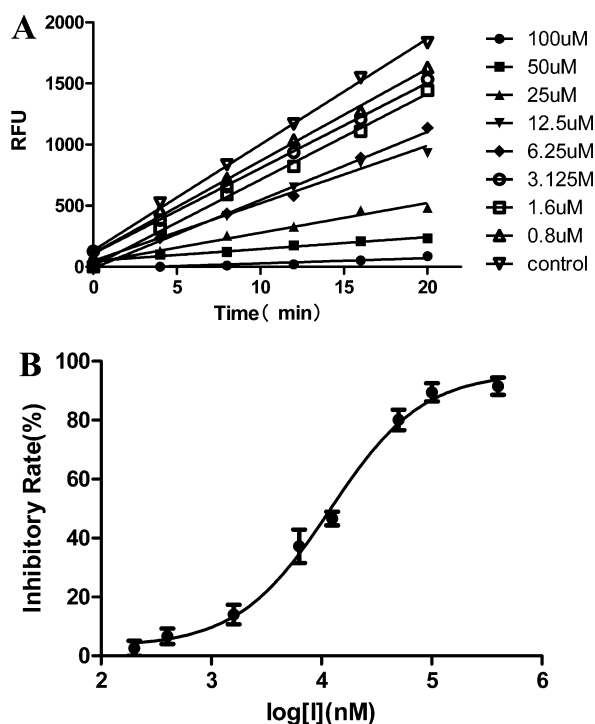
Figure 7. Compound **1** inhibited DENV-2 NS2B-NS3 protease activity in vitro. (A) Shown is the inhibitory progress curve of compound **1** in different concentrations ranging from 0.8 to 100 μM. (B) Compound **1** dose-dependently inhibited DENV-2 NS2B-NS3 protease in the cleavage of substrate Dabcyl-KQRRGRIE-Edans with IC$_{50}$ of 13.12 $\pm$ 1.03 μM.

Table 4. Antiviral Activities of the Compounds Tested

entry	compd	CC$_{50}$[a] (μM)	IC$_{50}$[b] (μM)	SI[c]
1	**1**	12.6	35.9	0.4
2	**22j**	29.7	8.0	3.7
3	**23b**	19.7	61.3	0.3
4	**23i**	>100	24.7	>4.1
5	**23j**	25	74.9	0.3
6	**23l**	16.4	73.4	0.2
7	**24g**	64.3	30.9	2.1
8	**24h**	49.7	11.0	4.5
9	curcumin	14.8	4.2	3.5
10	mycophenolic acid (MPA)	1.9	0.7	2.7

[a]CC$_{50}$ values were calculated with nontransfected cells. [b]IC$_{50}$ values were determined with the 96-well plate assay. [c]SI: selectivity index. SI = CC$_{50}$/IC$_{50}$.

24g,h) containing new scaffold (quinoline moiety) kept the moderate inhibitory activity against DENV NS2B-NS3 protease with IC$_{50}$ ranging from 7.46 $\pm$ 1.15 to 48.59 $\pm$ 3.46 μM (Tables 2 and 3). Values of two compounds **23d** (IC$_{50}$ = 7.83 $\pm$ 0.94 μM, Table 2) and **23g** (IC$_{50}$ = 7.46 $\pm$ 1.15 μM, Table 2) increased almost 2 times that of lead compound **1** (IC$_{50}$ = 13.12 $\pm$ 1.03 μM) in vitro. To our surprise, analogues **24a−h** with the same scaffold as **23a−m** but different side chain substitutions decreased the inhibitory activity (Table 3). Notably, the hit rate for inhibitors is 57% (12/21, defined as the number of active compounds divided by the number of compounds experimentally tested), higher than that of the first round (29%, 4/14), demonstrating that the scaffold hopping strategy employed in this study is efficient and valuable for discovering new DENV NS2B-NS3 protease inhibitors.

3.4.2. Antiviral Activity of Compounds 1, 22a,j,l,m, 23a−e,g−j,l, and 24g,h. To further validate the in vitro antiviral effects of these inhibitors, we constructed a subgenomic BHK-D2RepT-replicon (Figure 4) and compounds with in vitro inhibitory rate of more than 50% (**1, 22a, 22j, 22l,m, 23a−e, 23g−j, 23l,** and **24g,h**) have been evaluated on this DENV-2 luciferase reporter replicon-based assays (Table 4).

After virtual screening and chemical optimization, we tested in vitro antiviral activity of compound **1** and its derivatives **22a, 22j,** and **22l,m**. Only compound **22j** showed moderate activity against DENV (IC$_{50}$ = 8.0 μM, CC$_{50}$ = 29.7 μM, Table 4) among the derivatives tested. There is no big improvement on the antiviral activity compared to lead compound **1** (IC$_{50}$ = 35.9 μM, CC$_{50}$ = 12.6 μM, Table 4). This unsatisfactory result urged us to design new series of compounds **23** and **24**, obtained by scaffold hopping based on the common moiety of

compound **1** and its derivatives **22**. Of 12 compounds tested, six compounds showed antiviral activity with IC$_{50}$ ranging from 11.0 to 74.9 μM and their CC$_{50}$ ranging from 19.7 to >100 μM. We were delighted to observe a loss of cytotoxicity over DENV-2 luciferase reporter replicon with some compounds from this series (e.g., **23i** and **24h**), which demonstrated the efficiency of the strategy of scaffold hopping. The reason for loss of cytotoxicity might be attributed to the removal of one hydrazone substituent in the chemical structures of **23** and **24**.

3.5. SAR. The SAR analysis of a set of 36 compounds provided important insights into the essential structural requirement for effective dengue NS2B-NS3 protease inhibition. An analysis of the data shown in Tables 1−3 reveals some noteworthy observations of the SAR for compounds **1, 22a−l, 23a−m,** and **24a−h**: (1) It can be seen from compound **1** and its derivatives **22l−n**, obtained from structure-based virtual screening and subsequent chemical modification, respectively, that the absence of the double hydrazone substituents, phenolic hydroxyl, or carbethoxy on benzene ring causes these analogues to decrease antiviral activity (**1** vs **22l−n**) (see section 3.6). The presence of electron withdrawing groups on R$_3$ or R$_4$ improves the biological activity (**22a** vs **22j,k**), which urged us to use electron withdrawing groups on R$_5$ or R$_7$. (2) It can be observed from scaffold hopping that the high hit rate for inhibitors might be due to both the van der Waals and hydrogen bond interactions influenced by the quinoline ring and the hydrogen bond interactions on the carbonyl bond of the amide−hydrazine linker moiety of **23** and **24**, respectively (see section 3.6). (3) For compound **23g**, it was observed from modeling (see section 3.6) that the binding interaction between sulfonamide in R$_5$ and DENV NS2B-NS3 protease (such as Thr120 and Lys73) contribute to the inhibitory activity. Therefore, suggesting polar decoration on the R$_5$ or R$_7$ of the molecules may increase the biological activity (**23d, 23e, 23g, 23j, 23l, 24g,** and **24h**). (4) The analogues with two unsaturated bonds on the R$_6$ have better inhibitory activity (**23a** vs **23c** and **23e** vs **23g**). The effect of the linker length between hydrazide and phenyl is limited. (5) Between molecular series **23** and **24**, the former is better for the inhibitory activity of the derivatives. For derivates **24**, the significant loss of inhibitory activity may be attributable to a flexible acid amide chain (**24a** vs **23f, 24b** vs **23e, 24c** vs **23i, 24d** vs **23h, 24e** vs **23b, 24f** vs **23a**). It seems that more rigid substituents on R$_6$ or R$_8$ may contribute to the biological activity.
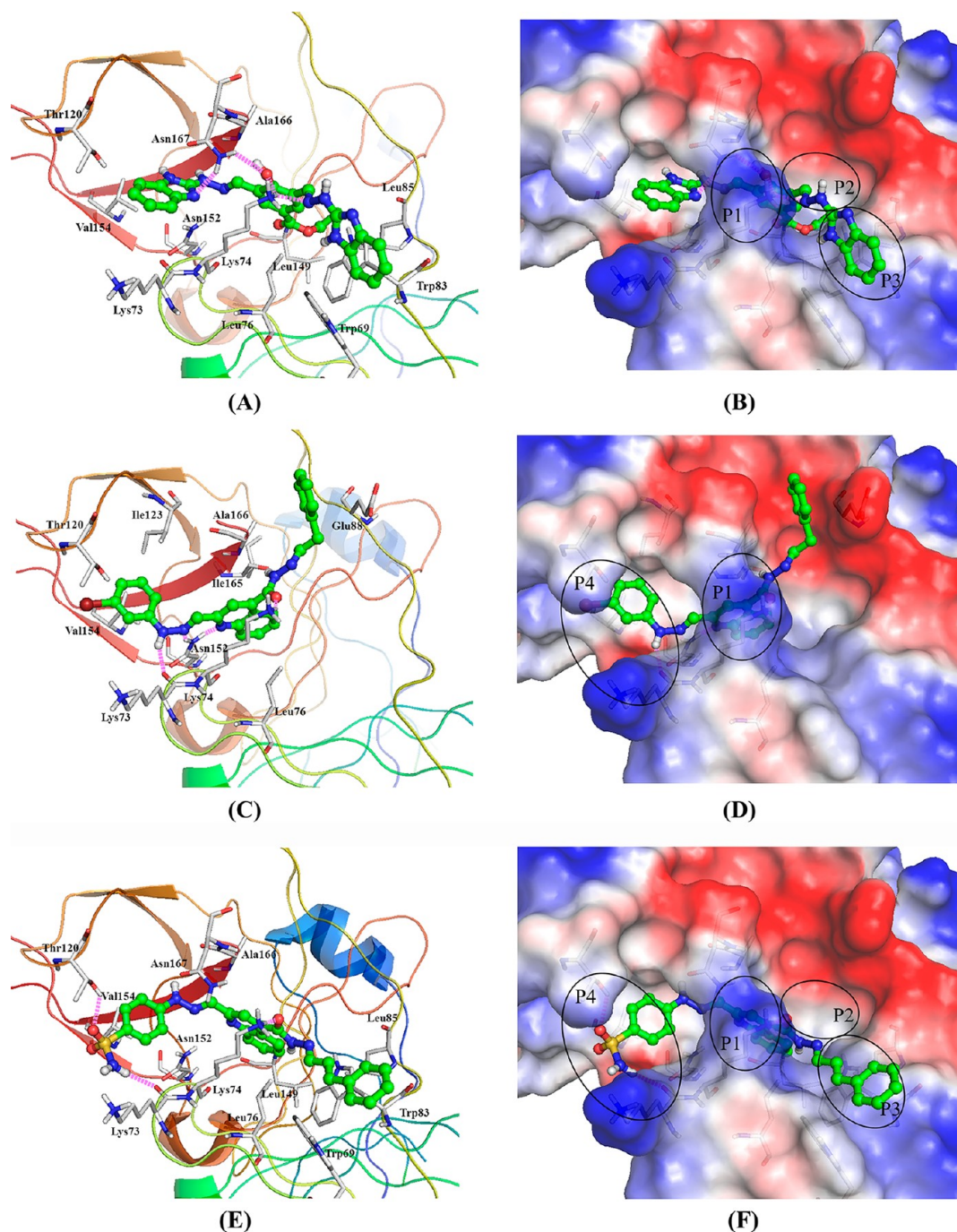
Figure 8. Three-dimensional (3D) interaction schemes of docked poses of **1** (A, B), **23i** (C, D) and **23g** (E, F) in the binding site of DENV-2 NS2B-NS3 protease. The poses were prepared using PyMol (http://pymol.sourceforge.net/). The ligands are shown as sticks, and the non-carbon atoms are colored by atom types (receptor carbon in white and ligand carbon in green). Hydrogen bonds are shown as dotted lines. The NS2B-NS3 surface is colored according to electrostatic potential. The subsites are labeled as P1, P2, P3, and P4.

3.6. Binding Models. To understand the structural basis for the binding affinities of the inhibitors for DENV NS2B-NS3 protease, we scrutinized the binding poses of compounds **1** and **23i**, obtained from virtual screening and scaffold hopping, respectively, by molecular docking (Figure 8A–D). For hit compound **1**, on the left side, the benzimidazole nitrogen form hydrogen-bonding interaction with side chain of Asn167 in the positive region P1 (Figure 8B), while phenol oxygen and the first nitrogen on hydrazone are involved in the hydrogen bonding network with the side chains of Asn167 and Lys74 (Figure 8A). On the right side, the benzimidazole moiety forms

hydrophobic interactions with Trp69 and Trp83 in the hydrophobic region P3 (Figure 8B). And the ester group has both hydrophobic and electrostatic interactions with the hydrophobic region P2 including residues of Leu85 and Leu149 (Figure 8B), which might explain the decrease of inhibitory activity observed in derivatives **22l–n**. For compound **23i**, the quinoline moiety has hydrophobic interactions with Leu76 and Ile165 (Figure 8C). On the left side, the first nitrogen on hydrazone and quinoline nitrogen form hydrogen-bonding interactions with Asn152 side chain (Figure 8C). The second nitrogen on the hydrazone also forms

hydrogen-bonding interaction with the carbonyl group of Lys73. The bromobenzene part is projected toward the hydrophobic region P4 consisting of hydrophobic residues, such as Ile123 and Val154 (Figure 8D). On the right side of the positive region P1, Lys74 is involved in tight hydrogen bonding with the carbonyl of the amide−hydrazine linker moiety of compound **23i**, while the amide−hydrazine nitrogen is observed to have hydrogen bonding with Ile165 main chain (Figure 8C). The phenyl part is sandwiched between the alkyl part of the Glu88 side chain and Ala166 side chain (Figure 8D). These interactions may explain that compound **23i** shows better inhibitory activity against DENV NS2B-NS3 protease than compound **1**. To further understand the electronic effects of the inhibitors, we scrutinized the binding hypothesis for the sulfonamide in R_5 of compound **23g**. It was observed that the sulfonamide in R_5 of **23g** could form more hydrogen bonds with the P4 region such as Thr120 and Lys73 (Figure 8E and Figure 8F), which might explain its higher inhibitory activity compared with others. These binding interactions gave insight into the structure optimization in a further study.

4. CONCLUSION

In summary, we have discovered novel small molecule inhibitors of DENV NS2B-NS3 protease using virtual screening and scaffold hopping techniques. Compound **1**, derived from the ACD database by virtual screening, was found against NS2B-NS3 protease activity. On the basis of the structure of lead compound **1**, 14 derivatives (**22a−n**) were designed, synthesized, and tested for inhibition activity. On the basis of the common scaffold of compound **1** and derivatives **22a−n**, we carried out scaffold hopping and identified a small compound (ZINC00036641) bearing quinoline as its core structure from the ZINC data set containing 60 000 small compounds. Twenty-one new compounds (**23a−m** and **24a−h**) containing new scaffold (quinoline moiety) were designed, synthesized, and evaluated for biological activity. In total, of 36 new compounds synthesized and tested, 17 compounds (**1**, **22a**, **22j**, **22l,m**, **23a−e**, **23g−j**, **23l**, and **24g,h**) were found to show DENV NS2B-NS3 protease inhibition activity and eight compounds (**1**, **22j**, **23b**, **23i,j**, **23l**, and **24g,h**) showed antiviral activity against DENV in vitro, which may be good leads for discovering new therapeutic agents for dengue viruses. Molecular binding models give rational explanations about SARs, which are in good agreement with pharmacological results. Discovering small molecule DENV NS2B-NS3 inhibitors is an urgent need, so the new chemical structures discovered in this study are of significance in terms of the chemical scaffold diversity. These findings have paved the way for the advancement of more potent compounds through rational drug design and optimization.

5. EXPERIMENTAL SECTION

Chemistry. General. The reagents (chemicals) were purchased from Lancaster, Alfa Aesar, J&K, Acros, and Shanghai Chemical Reagent Co. and used without further purification. Analytical thin-layer chromatography (TLC) was done with HSGF 254 (150−200 μm thickness; Yantai Huiyou Co., China). Reaction yields were not optimized. Melting points were measured in a capillary tube on a SGW X-4 melting point apparatus without correction. Nuclear magnetic resonance (NMR) spectroscopy was performed on a Bruker AMX-500 and AMX-400 NMR (IS as TMS) instrument. Chemical shifts were reported in parts per million (ppm, δ) downfield from tetramethylsilane. Proton coupling patterns were described as singlet (s), doublet (d), triplet (t), quartet (q), multiplet (m), and broad (br). Low- and

high-resolution mass spectrometry (LRMS and HRMS) conducted with electric, electrospray, and matrix-assisted laser desorption ionization (EI, ESI, and MALDI) produced by a Finnigan MAT-95, LCQ-DECA spectrometer and IonSpec 4.7 T. Compounds **1**, **22a−n**, **23a−m**, and **24a−h** were confirmed to have ≥95% purity (Supporting Information Table 1S). The details for purity analyses of these compounds are described in the Supporting Information.

Ethyl 4-Hydroxy-3,5-dimethylbenzoate (5). To a solution of 4-hydroxy-3,5-dimethylbenzoic acid (0.5 g) in 20 mL of EtOH was added 1 mL of H_2SO_4 (conc). The resulting reaction mixture was refluxed for 15 h. Solvent was removed under reduced pressure, and the residue was partitioned between EtOAc and saturated $NaHCO_3$ solution. The organic layer was washed with water and brine, dried over anhydrous Na_2SO_4, filtered, and condensed to give compound **5** as a white solid. Yield: 93%. Mp 116 °C. ^1H NMR (500 MHz, $CDCl_3$) δ: 1.36 (t, J = 7.1 Hz, 3H), 2.26 (s, 6H), 4.34 (q, J_1 = 7.1 Hz, J_2 = 14.3 Hz, 2H), 7.72 (s, 2H).

Ethyl 4-Acetoxy-3,5-dimethylbenzoate (6). A solution of **5** (160 mg) in acetic anhydride (Ac_2O, 5 mL) was heated at 140 °C for 18 h. Excess acetic anhydride and generated acetic acid were then evaporated under reduced pressure, and the residue was extracted with $EtOAc/H_2O$ three times. The combined organic layer was washed, dried, filtered, and condensed to give **6** as an orange solid. Yield: 82%. ^1H NMR (500 MHz, $CDCl_3$) δ: 1.36 (t, J = 7.1 Hz, 3H), 2.18 (s, 6H), 2.34 (s, 3H), 4.34 (q, J_1 = 7.1 Hz, J_2 = 14.3 Hz, 2H), 7.75 (s, 2H).

Ethyl 3,5-Bis(formyl)-4-hydroxybenzoate (7a) and Ethyl 3-Formyl-4-hydroxy-5-methylbenzoate (7b). A solution of the **6** (350 mg) in acetic anhydride (Ac_2O, 8 mL), acetic acid (8 mL, AcOH), and concentrated H_2SO_4 (1 mL) was cooled to 0 °C, and chromium trioxide (CrO_3, 0.69 g) was added in small portions during 2 h. After another 20 h, the reaction mixture was poured onto ice. Excess sodium metabisulfite solution was added, and it was extracted with EtOAc (3 × 20 mL). The organic layer was washed with water and brine, dried over anhydrous Na_2SO_4, filtered, and condensed. The residue was dissolved in EtOH (10 mL), and 100 μL of concentrated H_2SO_4 was added. The resulting reaction mixture was heated under reflux for 1 h. Solvent was removed under reduced pressure, and the residue was partitioned between EtOAc and saturated $NaHCO_3$. The organic layer was washed with water and brine, dried over anhydrous Na_2SO_4, filtered, and condensed. The residue was purified by chromatography on silica gel, eluting with EtOAc/petroleum ether (1:6, v/v) to give **7b** as a white solid. Yield: 20%. ^1H NMR (500 MHz, $CDCl_3$) δ: 1.40 (t, J = 7.2 Hz, 3H), 2.25 (s, 3H), 4.40 (q, J_1 = 7.2 Hz, J_2 = 14.4 Hz, 2H), 8.04 (s, 1H)), 8.15 (s, 1H), 9.95 (s, 1H). Further elution afforded **7a** as a yellow solid. Yield: 11%. ^1H NMR (500 MHz, $CDCl_3$) δ: 1.36 (t, J = 7.1 Hz, 3H), 4.40 (q, J_1 = 7.1 Hz, J_2 = 14.2 Hz, 2H), 8.52 (s, 2H), 10.30 (s, 2H). EI-MS m/z 222.1 (M⁺).

Ethyl 4-Hydroxy-3,5-bis((2-(1H-benzo[d]imidazol-2-yl)-hydrazinylidene)methyl)benzoate (1). To a solution of **7a** (75 mg, 0.34 mmol) in EtOH (5 mL) were added 1-(1H-benzimidazol-2-yl)hydrazine (110 mg, 0.74 mmol) (see Scheme 1 in Supporting Information) and AcOH (50 μL). The mixture was refluxed for 2 h. The reaction mixture was allowed to cool to room temperature and filtered. Then the precipitate was collected, washed with H_2O, and dried to afford **1** (107 mg, 65%) as a yellow solid. Mp >300 °C. ^1H NMR (500 MHz, DMSO-d_6) δ: 1.37 (t, J = 7.1 Hz, 3H), 4.36 (q, J_1 = 7.0 Hz, J_2 = 14.1 Hz, 2H), 7.00 (br, 4H), 7.22 (br, 4H), 8.25 (s, 2H), 8.42 (s, 2H), 11.55 (br, 4H), 12.23 (br, 1H). ESI-MS m/z 505.2 [M + Na]⁺. HRMS (ESI) m/z calcd for $C_{25}H_{22}N_8O_3$ [M + H]⁺ 483.1893, found 483.1879.

Ethyl 3-((2-(1H-Benzo[d]imidazol-2-yl)hydrazinylidene)-methyl)-4-hydroxy-5-methylbenzoate (22l). To a solution of **7b** (62 mg, 0.3 mmol) in EtOH (5 mL) were added 1-(1H-benzimidazol-2-yl)hydrazine (49 mg, 0.33 mmol) and AcOH (50 μL). The mixture was refluxed for 2 h. the reaction mixture was allowed to cool to room temperature and filtered. Then the precipitate was collected, washed with H_2O, and dried to afford **22l** (81 mg, 80%) as a yellow solid. Mp 279−282 °C. ^1H NMR (500 MHz, DMSO-d_6) δ: 1.31 (t, J = 7.1 Hz, 3H), 2.28 (s, 3H), 4.27 (q, J_1 = 7.1 Hz, J_2 = 14.2 Hz, 2H), 6.96 (br, 2H), 7.13 (br, 2H), 7.71 (s, 1H), 7.87 (s, 1H), 8.37 (s, 1H), 11.55 (br,

1H), 11.93 (br, 1H). EI-MS m/z 338.1 M$^+$. HRMS (ESI) m/z calcd for $C_{18}H_{18}N_4O_3$ [M + H]$^+$ 339.1457, found 339.1442.

Ethyl 4-Hydroxy-3,5-bis((2-(4-nitrophenyl)hydrazinylidene)-methyl)benzoate (22a). In the same manner as that described for the preparation of **1**, **22a** was prepared from **7a** and 4-nitrophenylhydrazine. Yield: 55%. Mp >300 °C. ^{1}H NMR (500 MHz, DMSO-d_6) δ: 1.37 (t, J = 7.2 Hz, 3H), 4.37 (q, J_1 = 7.2 Hz, J_2 = 14.4 Hz, 2H), 7.14 (d, J = 9.2 Hz, 4H), 8.20 (d, J = 9.2 Hz, 4H), 8.21 (s, 2H), 8.43 (s, 2H), 11.55 (s, 2H), 11.93 (s, 1H). EI-MS m/z 492.1 (M$^+$). HRMS (ESI) m/z calcd for $C_{23}H_{20}N_6O_7$ [M − H]$^−$ 491.1315, found 491.1345.

Ethyl 4-Hydroxy-3,5-bis((isoindoline-1,3-dione-2-yl-amino)-methylene)benzoate (22b). In the same manner as that described for the preparation of **1**, **22b** was prepared from **7a** and N-aminophthalimide. Yield: 60%. Mp 250−255 °C. ^{1}H NMR (500 MHz, DMSO-d_6) δ: 1.37 (t, J = 7.2 Hz, 3H), 4.32 (q, J_1 = 7.2 Hz, J_2 = 14.4 Hz, 2H), 7.82−7.84 (m, 2H), 7.90−7.92 (m, 3H), 7.96−7.98 (m, 3H), 8.58 (s, 2H), 9.72 (s, 2H), 12.79 (br, 1H). EI-MS m/z 510.2 (M$^+$). HRMS (ESI) m/z calcd for $C_{27}H_{18}N_4O_7$ [M + Na]$^+$ 533.1073, found 533.1063.

Ethyl 4-Hydroxy-3,5-bis((2-(pyridin-3-yl-carbonyl)-hydrazinylidene)methyl)benzoate (22c). In the same manner as that described for the preparation of **1**, **22c** was prepared from **7a** and nicotinic hydrazide. Yield: 53%. Mp 169−170 °C. ^{1}H NMR (500 MHz, DMSO-d_6) δ: 1.36 (t, J = 7.2 Hz, 3H), 4.37 (q, J_1 = 7.2 Hz, J_2 = 14.0 Hz, 2H), 7.58−7.61 (m, 3H), 8.28−8.31 (m, 2H), 8.37 (s, 2H), 8.79 (br, 3H), 9.12 (br, 2H), 12.45 (s, 2H), 13.28 (s, 1H). EI-MS m/z 460.2 (M$^+$). HRMS (ESI) m/z calcd for $C_{23}H_{20}N_6O_5$ [M + H]$^+$ 461.1573, found 461.1557.

Ethyl 4-Hydroxy-3,5-bis((2-(4-(aminosulfonyl)phenyl)-hydrazinylidene)methyl)benzoate (22d). In the same manner as that described for the preparation of **1**, **22d** was prepared from **7a** and 4-sulfonamidophenylhydrazine hydrochloride. Yield: 82%. Mp 242−248 °C. ^{1}H NMR (500 MHz, DMSO-d_6) δ: 1.37 (t, J = 7.2 Hz, 3H), 4.36 (q, J_1 = 7.2 Hz, J_2 = 14.0 Hz, 2H), 7.11 (d, J = 8.8 Hz, 8H), 7.73 (d, J = 8.8 Hz, 4H), 8.22 (s, 2H), 8.35 (s, 2H), 11.11 (s, 2H), 12.13 (s, 1H). EI-MS m/z 583.1 (M$^+$). HRMS (ESI) m/z calcd for $C_{23}H_{24}N_6O_7S_2$ [M + H]$^+$ 561.1226, found 561.1199.

Ethyl 4-Hydroxy-3,5-bis((2-(phenylcarbamoyl)-hydrazinylidene)methyl)benzoate (22e). In the same manner as that described for the preparation of **1**, **22e** was prepared from **7a** and 4-phenylsemicarbazide. Yield: 75%. Mp >300 °C. ^{1}H NMR (500 MHz, DMSO-d_6) δ: 1.36 (t, J = 6.8 Hz, 3H), 4.35 (q, J_1 = 7.2 Hz, J_2 = 14.4 Hz, 2H), 7.03 (t, J = 7.6 Hz, 2H), 7.31 (t, J = 7.6 Hz, 4H), 7.58 (d, J = 8.0 Hz, 4H), 8.33 (s, 2H), 8.38 (s, 2H), 9.07 (s, 2H), 10.79 (s, 2H), 12.32 (br, 1H). ESI-MS m/z 511.2 [M + Na]$^+$. HRMS (ESI) m/z calcd for $C_{25}H_{24}N_6O_5$ [M + Na]$^+$ 511.1706, found 511.1715.

Ethyl 4-Hydroxy-3,5-bis((2-carbamoylhydrazinyl)-methylene)benzoate (22f). In the same manner as that described for the preparation of **1**, **22f** was prepared from **7a** and semicarbazide. Yield: 54%. Mp 194−198 °C. ^{1}H NMR (500 MHz, DMSO-d_6) δ: 1.37 (t, J = 6.8 Hz, 3H), 4.32 (q, J_1 = 7.2 Hz, J_2 = 14.4 Hz, 2H), 7.24 (s, 2H), 7.72 (s, 2H), 8.31 (s, 6H), 8.42 (s, 2H). ESI-MS m/z 357.2 [M + Na]$^+$. HRMS (ESI) m/z calcd for $C_{13}H_{18}N_8O_3$ [M + H]$^+$ 335.1580, found 335.1566.

Ethyl 4-Hydroxy-3,5-bis((2-(ethylcarbamoyl)hydrazinyl)-methylene)benzoate (22g). In the same manner as that described for the preparation of **1**, **22g** was prepared from **7a** and 4-ethyl-3-thiosemicarbazide. Yield: 43%. Mp 263−265 °C. ^{1}H NMR (500 MHz, DMSO-d_6) δ: 1.17 (t, J = 7.2 Hz, 6H), 1.34 (t, J = 7.2 Hz, 3H), 3.56−3.63 (m, 4H), 4.34 (q, J_1 = 7.2 Hz, J_2 = 14.0 Hz, 2H), 8.27 (s, 2H), 8.42 (s, 2H), 8.64 (t, J = 4.8 Hz, 2H), 11.53 (s, 2H). EI-MS m/z 424.2 (M$^+$). HRMS (ESI) m/z calcd for $C_{17}H_{24}N_6O_3S_2$ [M + H]$^+$ 425.1430, found 425.1435.

Ethyl 4-Hydroxy-3,5-bis((2-carbamothioylhydrazinyl)-methylene)benzoate (22h). In the same manner as that described for the preparation of **1**, **22h** was prepared from **7a** and thiosemicarbazide. Yield: 54%. Mp 174−179 °C. ^{1}H NMR (500 MHz, DMSO-d_6) δ: 1.34 (t, J = 7.2 Hz, 6H), 4.33 (q, J_1 = 7.2 Hz, J_2 = 14.0 Hz, 2H), 8.16−8.28 (m, 5H), 8.42 (s, 2H), 11.56 (s, 2H). ESI-MS

m/z 391.3 [M + Na]$^+$. HRMS (ESI) m/z calcd for $C_{13}H_{16}N_6O_3S_2$ [M + Na]$^+$ 391.0623, found 391.0624.

Ethyl 4-Hydroxy-3,5-bis((2-(allylcarbamothioyl)hydrazinyl)-methylene)benzoate (22i). In the same manner as that described for the preparation of **1**, **22i** was prepared from **7a** and 4-allylthiosemicarbazide. Yield: 39%. Mp 250−253 °C. ^{1}H NMR (500 MHz, DMSO-d_6) δ: 1.37 (t, J = 7.2 Hz, 6H), 4.32 (t, J = 4.8 Hz, 4H), 4.34 (q, J_1 = 7.2 Hz, J_2 = 14.0 Hz, 2H), 5.12−5.16 (m, 4H), 5.82−5.98 (m, 2H), 8.26 (s, 2H), 8.43 (s, 2H), 8.84 (t, J = 4.8 Hz, 2H), 11.56 (s, 2H). ESI-MS m/z 449.2 [M + H]$^+$. HRMS (ESI) m/z calcd for $C_{19}H_{24}N_6O_3S_2$ [M + H]$^+$ 449.1430, found 449.1404.

Ethyl 4-Hydroxy-3,5-bis((2-(4-isopropylphenyl)-hydrazinylidene)methyl)benzoate (22j). In the same manner as that described for the preparation of **1**, **22j** was prepared from **7a** and 4-isopropylphenylhydrazine hydrochloride. Yield: 51%. Mp 262−264 °C. ^{1}H NMR (500 MHz, DMSO-d_6) δ: 1.19 (d, J = 6.8 Hz, 12H), 1.35 (t, J = 7.2 Hz, 3H), 2.79−2.84 (m, 2H), 4.35 (q, J_1 = 7.2 Hz, J_2 = 14.0 Hz, 2H), 6.95 (d, J = 8.4 Hz, 4H), 7.16 (d, J = 8.4 Hz, 4H), 8.12 (s, 2H), 8.22 (s, 2H), 10.54 (s, 2H), 12.45 (s, 1H). EI-MS m/z 486.3 (M$^+$). HRMS (ESI) m/z calcd for $C_{29}H_{34}N_4O_3$ [M + H]$^+$ 487.2709, found 487.2684.

Ethyl 4-Hydroxy-3,5-bis((2-(benzo[d][1,3]dioxol-5-carbonyl)-hydrazinylidene)methyl)benzoate (22k). In the same manner as that described for the preparation of **1**, **22k** was prepared from **7a** and benzo[d][1,3]dioxol-5-carbohydrazide. Yield: 81%. Mp 253−258 °C. ^{1}H NMR (500 MHz, DMSO-d_6) δ: 1.36 (t, J = 7.2 Hz, 3H), 4.38 (q, J_1 = 7.2 Hz, J_2 = 14.0 Hz, 2H), 6.15 (s, 4H), 7.19 (d, J = 8.0 Hz, 2H), 7.50 (s, 2H), 7.58 (d, J = 8.0 Hz, 2H), 8.33 (s, 2H), 8.77 (s, 2H), 12.14 (s, 2H), 13.40 (s, 1H). ESI-MS m/z 569.1 [M + Na]$^+$. HRMS (ESI) m/z calcd for $C_{27}H_{22}N_4O_9$ [M + Na]$^+$ 569.1284, found 569.1262.

Ethyl 3,5-Dimethylbenzoate (9). In the same manner as that described for the preparation of **5**, **9** was prepared from 3,5-dimethylbenzoic acid **8**. Yield: 98%. ^{1}H NMR (500 MHz, CDCl$_3$) δ: 1.36 (t, J = 7.2 Hz, 3H), 2.36 (s, 6H), 4.38 (q, J_1 = 7.2 Hz, J_2 = 14.0 Hz, 2H), 7.18 (s, 1H), 7.72 (s, 2H).

Ethyl 3,5-Diformylbenzoate (12). In the same manner as that described for the preparation of **9a**, **12** was prepared from **11**. Yield: 28%. ^{1}H NMR (500 MHz, CDCl$_3$) δ: 1.46 (t, J = 7.2 Hz, 3H), 2.36 (s, 6H), 4.50 (q, J_1 = 7.2 Hz, J_2 = 14.0 Hz, 2H), 8.56 (t, J = 7.8 Hz, 1H), 8.79 (d, J = 7.8 Hz, 2H), 10.19 (s, 2H). EI-MS m/z 206.1 (M$^+$).

Ethyl 3,5-Bis((2-(1H-benzo[d]imidazol-2-yl)hydrazinylidene)-methyl)benzoate (22m). In the same manner as that described for the preparation of **1**, **22m** was prepared from **10** and 1-(1H-benzimidazol-2-yl)hydrazine. Yield: 37%. Mp 312−315 °C. ^{1}H NMR (500 MHz, DMSO-d_6) δ: 1.37 (t, J = 7.2 Hz, 3H), 4.32 (q, J = 7.2 Hz, J_2 = 14.0 Hz, 2H), 6.90−7.00 (m, 4H), 7.24−7.27 (m, 4H), 8.15 (s, 2H), 8.27 (s, 2H), 8.38 (s, 1H), 8.40 (s, 1H), 8.47 (s, 1H), 8.56 (s, 1H). EI-MS m/z 466.2 (M$^+$). HRMS (ESI) m/z calcd for $C_{25}H_{22}N_8O_2$ [M + H]$^+$ 467.1944, found 467.1923.

2,6-Dimethylphenyl Acetate (12). In the same manner as that described for the preparation of **6**, **12** was prepared from **11**. Yield: 88%. ^{1}H NMR (500 MHz, CDCl$_3$) δ: 2.19 (s, 6H), 2.36 (s, 3H), 7.09−7.15 (m, 3H).

2-Hydroxybenzene-1,3-dialdehyde (13). In the same manner as that described for the preparation of **7a**, **13** was prepared from **12**. Yield: 30%. ^{1}H NMR (500 MHz, CDCl$_3$) δ: 6.94 (t, J = 7.6 Hz, 1H), 7.41 (d, J = 7.6 Hz, 2H), 9.89 (s, 2H), 11.27 (s, 1H).

2-Hydroxyisophthalaldehyde-1,3-bis(2-(1H-benzo[d]-imidazol)hydrazone) (22n). In the same manner as that described for the preparation of **1**, **22n** was prepared from **13** and 1-(1H-benzimidazol-2-yl)hydrazine. Yield: 66%. Mp >300 °C. ^{1}H NMR (500 MHz, DMSO-d_6) δ: 6.96−7.00 (m, 4H), 7.12 (t, J = 8.0 Hz, 1H), 7.20−7.22 (m, 4H), 7.74 (d, J = 8.0 Hz, 2H), 8.40 (s, 2H), 10.26 (s, 1H), 10.47 (s, 2H), 11.44 (br, 2H). EI-MS m/z 410.2 (M$^+$). HRMS (ESI) m/z calcd for $C_{22}H_{18}N_8O$ [M + H]$^+$ 411.1682, found 411.1658.

2-Methylquinoline-4-carboxylic Acid (15). A mixture of isatin **14** (1.0 g, 6.8 mmol) and 85% aqueous potassium hydroxide (2.67 g, 47.6 mmol) was heated to 50 °C for 40 min. Acetone (5 mL, 56.7 mmol) was then added dropwise, maintaining the temperature at 50 °C. After being stirred for 15 h, the reaction mixture was cooled to

room temperature and acidified to pH 3 by addition of concentrated HCl to obtain a heavy slurry which was filtered, washed, and dried to afford 2-methylquinoline-4-carboxylic acid **15** (1.0 g, 79%) as a white solid. Mp 248−250 °C. ^{1}H NMR (400 MHz, DMSO-d_6): δ 2.72 (s, 3H), 7.64 (t, J = 8.0 Hz, 1H), 7.78 (t, J = 8.0 Hz, 1H), 7.84 (s, 1H), 8.02 (d, J = 8.4 Hz, 1H), 8.63 (d, J = 8.4 Hz, 1H).

Ethyl 2-Methylquinoline-4-carboxylate (16). In the same manner as that described for the preparation of **5**, **16** was prepared from **15**. Yield: 80%. ^{1}H NMR (400 MHz, CDCl$_3$) δ 1.50 (t, J = 7.2 Hz, 3H), 2.83 (s, 3H), 4.53 (q, J_1 = 7.2 Hz, J_2 = 14.0 Hz, 2H), 7.61 (t, J = 8.0 Hz, 1H), 7.76 (t, J = 8.0 Hz, 1H), 7.82 (s, 1H), 8.10 (d, J = 8.4 Hz, 1H), 8.71 (d, J = 8.4 Hz, 1H).

Ethyl 2-Formylquinoline-4-carboxylate (17). To a solution of **16** (0.5 g) in 10 mL of dioxane, selenium dioxide (SeO$_2$, 1.3 g) was added. The resulting reaction mixture was reflux for 4 h. Solvent was removed under reduced pressure, and the residue was extracted with EtOAc/H$_2$O. The organic layer was washed with water and brine, dried over anhydrous Na$_2$SO$_4$, filtered, and condensed. The residue was purified by chromatography on silica gel, eluting with a mixture of EtOAc/petroleum ether (1:4, v/v) to give **17** as a pale yellow solid. Yield: 99%. ^{1}H NMR (400 MHz, CDCl$_3$): δ 1.52 (t, J = 7.2 Hz, 3H), 4.56 (q, J_1 = 7.2 Hz, J_2 = 14.0 Hz, 2H), 7.83 (t, J = 8.0 Hz, 1H), 7.91 (t, J = 8.0 Hz, 1H), 8.35 (d, J = 8.0 Hz, 1H), 8.54 (s, 1H), 8.90 (d, J = 8.0 Hz, 1H), 10.29 (s, 1H).

Ethyl 2-((2-(3-Chlorophenyl)hydrazinylidene)methyl)-quinoline-4-carboxylate (18a). To a solution of **17** (23 mg, 0.1 mmol) in EtOH (5 mL) were added 3-chlorophenylhydrazine hydrochloride (22 mg, 0.12 mmol) and AcOH (50 μL). The mixture was refluxed for 2 h. The reaction mixture was allowed to cool to room temperature and filtered. Then the precipitate was collected, washed with H$_2$O, and dried to afford **18a** (26 mg, 75%) as a yellow solid. ^{1}H NMR (400 MHz, DMSO-d_6) δ: 1.44 (t, J = 7.6 Hz, 3H), 4.53 (q, J_1 = 7.2 Hz, J_2 = 14.4 Hz, 2H), 6.96 (d, J = 8.0 Hz, 1H), 7.18 (d, J = 8.0 Hz, 1H), 7.31−7.37 (m, 2H), 7.75 (t, J = 8.0 Hz, 1H), 7.91 (t, J = 7.6 Hz, 1H), 8.17 (d, J = 8.4 Hz, 1H), 8.25 (s, 1H), 8.52 (d, J = 8.4 Hz, 1H), 8.55 (s, 1H), 11.88 (br, 1H).

Ethyl 2-((2-(4-(Aminosulfonyl)phenyl)hydrazinylidene)-methyl)quinoline-4-carboxylate (18b). In the same manner as that described for the preparation of **18a**, **18b** was prepared from **17** and 4-sulfonamidophenylhydrazine hydrochloride. Yield: 75%. ^{1}H NMR (400 MHz, DMSO-d_6) δ 1.45 (t, J = 7.2 Hz, 3H), 4.52 (q, J_1 = 7.2 Hz, J_2 = 14.0 Hz, 2H), 7.17 (s, 2H), 7.29 (d, J = 8.8 Hz, 2H), 7.70 (t, J = 8.0 Hz, 1H), 7.76 (d, J = 8.4 Hz, 2H), 7.85 (t, J = 8.0 Hz, 1H), 8.09 (d, J = 8.4 Hz, 1H), 8.15 (s, 1H), 8.48 (s, 1H), 8.52 (d, J = 8.4 Hz, 1H), 11.42 (s, 1H).

Ethyl 2-((2-(3-Bromophenyl)hydrazinylidene)methyl)-quinoline-4-carboxylate (18c). In the same manner as that described for the preparation of **18a**, **18c** was prepared from **17** and 3-bromophenylhydrazine hydrochloride. Yield: 65%. ^{1}H NMR (400 MHz, DMSO-d_6) δ 1.45 (t, J = 7.2 Hz, 3H), 4.53 (q, J_1 = 7.2 Hz, J_2 = 14.0 Hz, 2H), 7.08 (d, J = 7.6 Hz, 1H), 7.20 (d, J = 8.0 Hz, 1H), 7.28 (t, J = 8.0 Hz, 1H), 7.44 (s, 1H), 7.75 (t, J = 7.6 Hz, 1H), 7.90 (t, J = 7.6 Hz, 1H), 8.15 (d, J = 8.0 Hz, 1H), 8.21 (s, 1H), 8.52−8.53 (m, 2H), 11.73 (br, 1H).

Ethyl 2-((2-(3-Nitrophenyl)hydrazinylidene)methyl)-quinoline-4-carboxylate (18d). In the same manner as that described for the preparation of **18a**, **18d** was prepared from **17** and 3-nitrophenylhydrazine hydrochloride. Yield: 60%. ^{1}H NMR (400 MHz, DMSO-d_6) δ 1.45 (t, J = 7.2 Hz, 3H), 4.52 (q, J_1 = 7.2 Hz, J_2 = 14.0 Hz, 2H), 7.18 (d, J = 7.6 Hz, 1H), 7.23 (d, J = 8.0 Hz, 1H), 7.28 (t, J = 8.0 Hz, 1H), 7.54 (s, 1H), 7.78 (t, J = 7.6 Hz, 1H), 7.94 (t, J = 7.6 Hz, 1H), 8.35 (d, J = 8.0 Hz, 1H), 8.34 (s, 1H), 8.72 (d, J = 8.4 Hz, 1H), 11.53 (br, 1H).

Ethyl 2-((2-(3-(Trifluoromethyl)phenyl)hydrazinylidene)-methyl)quinoline-4-carboxylate (18e). In the same manner as that described for the preparation of **18a**, **18e** was prepared from **17** and 3-(trifluoromethyl)phenylhydrazine. Yield: 65%. EI-MS m/z 387.2 (M$^+$).

2-((2-(3-Chlorophenyl)hydrazinylidene)methyl)quinoline-4-carbohydrazide (19a). **18a** (25 mg, 0.07 mmol) was slowly added to

the hydrazine hydrate (2.5 mL). The reaction mixture was heated to 120 °C for 20 h. After being cooled to about 20 °C, it was poured into ice−water. The resulting crystals were collected after filtration and washed with water and dried to afford compound **19a** (22 mg, 90%) as a yellow solid. EI-MS m/z 339.1 (M$^+$).

2-((2-(4-(Aminosulfonyl)phenyl)hydrazinylidene)methyl)-quinoline-4-carbohydrazide (19b). In the same manner as that described for the preparation of **19a**, **19b** was prepared from **18b** and hydrazine hydrate. Yield: 95%. ^{1}H NMR (400 MHz, DMSO-d_6) δ 4.73 (br, 2H), 7.21 (br, 2H), 7.55 (d, J = 8.4 Hz, 2H), 7.62 (s, 1H), 7.72−7.80 (m, 4H), 7.92 (t, J = 7.2 Hz, 1H), 8.17 (d, J = 8.0 Hz, 1H), 8.44 (d, J = 8.0 Hz, 1H), 10.00 (br, 1H), 14.77 (s, 1H).

2-((2-(3-Bromophenyl)hydrazinylidene)methyl)quinoline-4-carbohydrazide (19c). In the same manner as that described for the preparation of **19a**, **19c** was prepared from **18c** and hydrazine hydrate. Yield: 88%. EI-MS m/z 383.0 (M$^+$).

2-((2-(3-Nitrophenyl)hydrazinylidene)methyl)quinoline-4-carbohydrazide (19d). In the same manner as that described for the preparation of **19a**, **19d** was prepared from **18d** and hydrazine hydrate. Yield: 98%. ^{1}H NMR (400 MHz, DMSO-d_6) δ 4.71 (br, 2H), 6.35 (d, J = 8.0 Hz, 1H), 6.61 (d, J = 8.0 Hz, 1H), 7.75 (s, 1H), 7.07 (t, J = 8.0 Hz, 1H), 7.58 (t, J = 8.0 Hz, 1H), 7.77 (t, J = 7.6 Hz, 1H), 7.98−8.08 (m, 4H), 8.30 (br, 2H), 10.00 (br, 1H), 10.91 (s, 1H).

2-((2-(3-(Trifluoromethyl)phenyl)hydrazinylidene)methyl)-quinoline-4-carbohydrazide (19e). In the same manner as that described for the preparation of **19a**, **19e** was prepared from **18e** and hydrazine hydrate. Yield: 87%. EI-MS m/z 373.1 (M$^+$).

2-((2-(3-Chlorophenyl)hydrazinylidene)methyl)-N'-(3-phenylpropylidene)quinoline-4-carbohydrazide (23a). To a solution of **19a** (80 mg, 0.23 mmol) in EtOH (5 mL) were added phenylpropyl aldehyde (62 mg, 0.46 mmol) and AcOH (50 μL). The mixture was refluxed for 2 h. The reaction mixture was allowed to cool to room temperature and filtered. Then the precipitate was collected, washed with H$_2$O, and dried to afford **23a** (78 mg, 75%) as a yellow solid. Mp 266−268 °C. ^{1}H NMR (400 MHz, DMSO-d_6) δ: 2.62−2.67 (m, 2H), 2.88 (t, J = 8.0 Hz, 2H), 7.14 (d, J = 8.0 Hz, 1H), 7.22−7.29 (m, 7H), 7.63 (t, J = 8.0 Hz, 1H), 7.73 (t, J = 8.0 Hz, 1H), 7.79 (t, J = 8.0 Hz, 1H), 8.03−8.08 (m, 4H), 8.19 (s, 1H), 11.17 (s, 1H), 11.90 (s, 1H). ESI-MS m/z 456.2 [M + H]$^+$. HRMS (ESI) m/z calcd for C$_{26}$H$_{22}$ClN$_5$O [M + H]$^+$ 456.1591, found 456.1586.

2-((2-(3-Chlorophenyl)hydrazinylidene)methyl)-N'-(2-phenylethylidene)quinoline-4-carbohydrazide (23b). In the same manner as that described for the preparation of **23a**, **23b** was prepared from **19a** and phenylacetaldehyde. Yield: 57%. Mp 255 °C. ^{1}H NMR (400 MHz, DMSO-d_6) δ: 3.69 (d, J = 6.0 Hz, 2H), 6.88 (d, J = 7.6 Hz, 1H), 7.14 (d, J = 8.4 Hz, 1H), 7.25−7.40 (m, 7H), 7.63 (t, J = 7.6 Hz, 1H), 7.77−7.82 (m, 2H), 8.03−8.08 (m, 3H), 8.22 (s, 1H), 11.16 (s, 1H), 11.95 (s, 1H). ESI-MS m/z 442.2 [M + H]$^+$. HRMS (ESI) m/z calcd for C$_{25}$H$_{20}$ClN$_5$O [M + H]$^+$ 442.1435, found 442.1448.

2-((2-(3-Chlorophenyl)hydrazinylidene)methyl)-N'-((E)-3-phenylallylidene)quinoline-4-carbohydrazide (23c). In the same manner as that described for the preparation of **23a**, **23c** was prepared from **19a** and cinnamaldehyde. Yield: 66%. Mp 272 °C. ^{1}H NMR (400 MHz, DMSO-d_6) δ: 6.88 (d, J = 8.0 Hz, 2H), 7.13−7.37 (m, 7H), 7.42 (t, J = 7.2 Hz, 1H), 7.66 (d, J = 7.6 Hz, 2H), 7.82 (t, J = 7.2 Hz, 1H), 8.05−8.11 (m, 3H), 8.17−8.18 (m, 1H), 8.28 (s, 1H), 11.18 (s, 1H), 12.17 (s, 1H). ESI-MS m/z 454.2 [M + H]$^+$. HRMS (ESI) m/z calcd for C$_{26}$H$_{20}$ClN$_5$O [M + H]$^+$ 454.1435, found 454.1448.

2-((2-(4-Aminosulfonylphenyl)hydrazinylidene)methyl)-N'-(3-hydroxybenzylidene)quinoline-4-carbohydrazide (23d). In the same manner as that described for the preparation of **23a**, **23d** was prepared from **19b** and 3-hydroxybenzaldehyde. Yield: 90%. Mp 252−253 °C. ^{1}H NMR (400 MHz, DMSO-d_6) δ: 7.15 (t, J = 7.6 Hz, 3H), 7.29 (d, J = 8.4 Hz, 2H), 7.35 (d, J = 8.4 Hz, 2H), 7.66−7.85 (m, 4H), 8.06−8.15 (m, 2H), 8.17 (s, 1H), 8.29 (s, 1H), 8.32 (s, 1H), 9.69 (s, 1H), 11.39 (s, 1H), 12.24 (s, 1H). ESI-MS m/z 489.2 [M + H]$^+$. HRMS (ESI) m/z calcd for C$_{24}$H$_{20}$N$_6$O$_4$S [M + H]$^+$ 489.1345, found 489.1356.

2-((2-(4-Aminosulfonylphenyl)hydrazinylidene)methyl)-N'-(3-phenylpropylidene)quinoline-4-carbohydrazide (23e). In

the same manner as that described for the preparation of **23a**, **23e** was prepared from **19b** and phenylpropyl aldehyde. Yield: 58%. Mp 260−261 °C. ^{1}H NMR (400 MHz, DMSO-d_6) δ: 2.63−2.66 (m, 2H), 2.87 (t, J = 8.0 Hz, 2H), 7.24−7.33 (m, 7H), 7.56 (d, J = 8.0 Hz, 2H), 7.70−7.80 (m, 5H), 7.93−7.98 (m, 2H), 8.12 (d, J = 8.0 Hz, 1H), 8.47 (d, J = 8.0 Hz, 1H), 11.96 (s, 1H), 14.77 (s, 1H). ESI-MS m/z 501.2 [M + H]$^+$. HRMS (ESI) m/z calcd for $C_{26}H_{24}N_6O_3S$ [M + H]$^+$ 501.1709, found 501.1702.

2-((2-(4-Aminosulfonylphenyl)hydrazinylidene)methyl)-N'-(2-phenylethylidene)quinoline-4-carbohydrazide (23f). In the same manner as that described for the preparation of **23a**, **23f** was prepared from **19b** and phenylacetaldehyde. Yield: 67%. Mp 257 °C. ^{1}H NMR (400 MHz, DMSO-d_6) δ: 3.69 (d, J = 6.0 Hz, 2H), 7.21 (s, 2H), 7.27−7.40 (m, 5H), 7.55 (d, J = 8.8 Hz, 2H), 7.62 (s, 1H), 7.72−7.84 (m, 5H), 7.92−7.95 (m, 2H), 8.45 (t, J = 8.0 Hz, 1H), 11.98 (s, 1H), 14.75 (s, 1H). ESI-MS m/z 487.2 [M + H]$^+$. HRMS (ESI) m/z calcd for $C_{25}H_{22}N_6O_3S$ [M + H]$^+$ 487.1552, found 487.1562.

2-((2-(4-Aminosulfonylphenyl)hydrazinylidene)methyl)-N'-((E)-3-phenylallylidene)quinoline-4-carbohydrazide (23g). In the same manner as that described for the preparation of **23a**, **23g** was prepared from **19b** and cinnamaldehyde. Yield: 90%. Mp 264 °C. ^{1}H NMR (400 MHz, DMSO-d_6) δ: 7.14 (d, J = 8.0 Hz, 1H), 7.22 (s, 2H), 7.27 (t, J = 8.0 Hz, 1H), 7.38 (t, J = 7.6 Hz, 1H), 7.42 (t, J = 7.6 Hz, 1H), 7.57 (d, J = 8.0 Hz, 2H), 7.66 (t, J = 8.0 Hz, 2H), 7.73−7.85 (m, 4H), 7.91−8.00 (m, 2H), 8.16 (t, J = 7.6 Hz, 1H), 8.47 (t, J = 7.6 Hz, 1H), 12.19 (s, 1H), 14.77 (s, 1H). ESI-MS m/z 499.2 [M + H]$^+$. HRMS (ESI) m/z calcd for $C_{26}H_{22}N_6O_3S$ [M + H]$^+$ 499.1552, found 499.1565.

2-((2-(3-Bromophenyl)hydrazinylidene)methyl)-N'-(3-phenylpropylidene)quinoline-4-carbohydrazide (23h). In the same manner as that described for the preparation of **23a**, **23h** was prepared from **19c** and phenylpropyl aldehyde. Yield: 78%. Mp 265−267 °C. ^{1}H NMR (400 MHz, DMSO-d_6) δ: 2.62−2.67 (m, 2H), 2.88 (t, J = 8.0 Hz, 2H), 7.02 (d, J = 8.0 Hz, 1H), 7.18−7.33 (m, 7H), 7.63 (t, J = 8.0 Hz, 1H), 7.73 (t, J = 8.0 Hz, 1H), 7.81 (t, J = 8.0 Hz, 1H), 8.02−8.08 (m, 4H), 8.18 (s, 1H), 11.15 (s, 1H), 11.91 (s, 1H). ESI-MS m/z 500.2 [M + H]$^+$. HRMS (ESI) m/z calcd for $C_{26}H_{22}BrN_5O$ [M + H]$^+$ 500.1086, found 500.1100.

2-((2-(3-Bromophenyl)hydrazinylidene)methyl)-N'-(2-phenylethylidene)quinoline-4-carbohydrazide (23i). In the same manner as that described for the preparation of **23a**, **23i** was prepared from **19c** and phenylacetaldehyde. Yield: 73%. Mp 258 °C. ^{1}H NMR (400 MHz, DMSO-d_6) δ: 3.69 (d, J = 6.0 Hz, 2H), 7.02 (br, 1H), 7.18−7.40 (m, 8H), 7.63 (t, J = 8.0 Hz, 1H), 7.77−7.83 (m, 2H), 8.03−8.07 (m, 3H), 8.21 (s, 1H), 11.14 (s, 1H), 11.95 (s, 1H). ESI-MS m/z 486.1 [M + H]$^+$. HRMS (ESI) m/z calcd for $C_{25}H_{20}BrN_5O$ [M + H]$^+$ 486.0929, found 486.0944.

2-((2-(3-Nitrophenyl)hydrazinylidene)methyl)-N'-((E)-3-phenylallylidene)quinoline-4-carbohydrazide (23j). In the same manner as that described for the preparation of **23a**, **23j** was prepared from **19d** and cinnamaldehyde. Yield: 56%. Mp 232 °C. ^{1}H NMR (400 MHz, DMSO-d_6) δ: 7.11−7.14 (m, 1H), 7.25−7.43 (m, 8H), 7.62−7.82 (m, 6H), 8.05−8.19 (m, 3H), 11.35 (s, 1H), 12.24 (s, 1H). ESI-MS m/z 465.2 [M + H]$^+$. HRMS (ESI) m/z calcd for $C_{26}H_{20}N_6O_3$ [M + H]$^+$ 465.1675, found 465.1648.

2-((2-(3-(Trifluoromethyl)phenyl)hydrazinylidene)methyl)-N'-(3-phenylpropylidene)quinoline-4-carbohydrazide (23k). In the same manner as that described for the preparation of **23a**, **23k** was prepared from **19e** and phenylpropyl aldehyde. Yield: 93%. Mp 268−275 °C. ^{1}H NMR (400 MHz, DMSO-d_6) δ: 2.62−2.67 (m, 2H), 2.88 (t, J = 8.0 Hz, 2H), 7.03−7.09 (m, 1H), 7.18−7.24 (m, 2H), 7.29−7.34 (m, 3H), 7.42−7.53 (m, 3H), 7.64 (t, J = 8.0 Hz, 1H), 7.72 (t, J = 8.0 Hz, 1H), 7.82 (t, J = 8.0 Hz, 1H), 8.03−8.06 (m, 2H), 8.12 (s, 1H), 8.19 (s, 1H), 11.31 (s, 1H), 11.93 (s, 1H). ESI-MS m/z 490.2 [M + H]$^+$. HRMS (ESI) m/z calcd for $C_{27}H_{22}F_3N_5O$ [M + H]$^+$ 490.1855, found 490.1873.

2-((2-(3-(Trifluoromethyl)phenyl)hydrazinylidene)methyl)-N'-(2-phenylethylidene)quinoline-4-carbohydrazide (23l). In the same manner as that described for the preparation of **23a**, **23l** was prepared from **19e** and phenylacetaldehyde. Yield: 56%. Mp 272

°C. ^{1}H NMR (400 MHz, DMSO-d_6) δ: 3.69 (d, J = 5.6 Hz, 2H), 7.17 (d, J = 5.2 Hz, 2H), 7.31−7.38 (m, 4H), 7.44 (s, 1H), 7.51−7.54 (m, 2H), 7.64 (t, J = 7.2 Hz, 1H), 7.77−7.83 (m, 2H), 8.04−8.08 (m, 2H), 8.11 (s, 1H), 8.22 (s, 1H), 11.29 (s, 1H), 11.97 (s, 1H). ESI-MS m/z 476.2 [M + H]$^+$. HRMS (ESI) m/z calcd for $C_{26}H_{20}F_3N_5O$ [M + H]$^+$ 476.1698, found 476.1714.

2-((2-(3-(Trifluoromethyl)phenyl)hydrazinylidene)methyl)-N'-((E)-3-phenylallylidene)quinoline-4-carbohydrazide (23m). In the same manner as that described for the preparation of **23a**, **23m** was prepared from **19e** and cinnamaldehyde. Yield: 86%. Mp 276 °C. ^{1}H NMR (400 MHz, DMSO-d_6) δ: 7.13 (t, J = 8.0 Hz, 2H), 7.40−7.58 (m, 6H), 7.66 (d, J = 8.0 Hz, 2H), 7.76−7.85 (m, 2H), 8.06−8.18 (m, 5H), 8.28 (s, 1H), 11.32 (s, 1H), 12.19 (s, 1H). ESI-MS m/z 488.2 [M + H]$^+$. HRMS (ESI) m/z calcd for $C_{27}H_{20}F_3N_5O$ [M + H]$^+$ 488.1698, found 488.1714.

2-Formylquinoline-4-carboxylic Acid (20). To a solution of **15** (0.37 g) in 3 mL of dioxane, selenium dioxide (SeO$_2$, 1.11 g) was added. The resulting reaction mixture was heated to 40 °C for 15 h. Solvent was removed under reduced pressure, and the residue was extracted with EtOAc/H$_2$O. The organic layer was washed with water and brine, dried over anhydrous Na$_2$SO$_4$, filtered, and condensed. The residue was purified by chromatography with DCM/MeOH (5:1, v/v) to give **20** as a yellow solid. Yield: 56%. ^{1}H NMR (400 MHz, DMSO-d_6): δ 7.93 (t, J = 8.0 Hz, 1H), 8.00 (t, J = 8.0 Hz, 1H), 8.32 (s, 1H), 8.33 (d, J = 8.0 Hz, 1H), 8.82 (d, J = 8.0 Hz, 1H), 10.16 (s, 1H).

2-Formyl-N-(3-phenylpropyl)quinoline-4-carboxamide (21a). Into a solution of **20** (75 mg, 0.37 mmol) in methylene chloride (DCM, 10 mL) were added EDCI (216 mg, 1.12 mmol) and HOBt (203 mg, 1.5 mmol). After the mixture was stirred for 1 h at 0 °C, a solution of the triethylamine (TEA, 400 μL) and 3-phenylpropan-1-amine (78 mg, 0.56 mmol) in DCM (2 mL) was added dropwise. The resulting mixture was stirred at room temperature overnight. The solvent was removed under reduced pressure, and the residue was extracted with EtOAc/H$_2$O. The organic layer was washed with 2 N aqueous HCl, saturated NaHCO$_3$, brine and then dried over anhydrous Na$_2$SO$_4$, filtered, and condensed. The residue was purified by chromatography on silica gel, eluting with a mixture of EtOAc/petroleum ether (1:4, v/v) to give **21a** as a white solid. Yield: 70%. ^{1}H NMR (400 MHz, CDCl$_3$): δ 2.07 (t, J = 7.2 Hz, 2H), 2.77−2.82 (m, 2H), 3.62 (t, J = 6.8 Hz, 2H), 7.23−7.32 (m, 5H), 7.77 (t, J = 7.2 Hz, 1H), 7.88 (t, J = 7.6 Hz, 1H), 7.96 (s, 1H), 8.29 (d, J = 8.4 Hz, 1H), 8.36 (d, J = 8.4 Hz, 1H), 10.23 (s, 1H).

2-Formyl-N-(4-phenylbutyl)quinoline-4-carboxamide (21b). In the same manner as that described for the preparation of **21a**, **21b** was prepared from **20** and 4-phenylbutan-1-amine. Yield: 86%. ^{1}H NMR (400 MHz, CDCl$_3$) δ: 1.63−1.73 (m, 4H), 2.67 (t, J = 6.8 Hz, 2H), 3.41−3.45 (m, 2H), 7.23−7.32 (m, 5H), 7.76 (t, J = 7.2 Hz, 1H), 7.88 (t, J = 7.6 Hz, 1H), 7.94 (s, 1H), 8.26 (d, J = 8.4 Hz, 1H), 8.29 (d, J = 8.4 Hz, 1H), 10.24 (s, 1H).

2-((2-(4-(Aminosulfonyl)phenyl)hydrazinylidene)methyl)-N-(3-phenylpropyl)quinoline-4-carboxamide (24a). To a solution of **21a** (40 mg, 0.13 mmol) in EtOH (5 mL) were added 4-sulfonamidophenylhydrazine hydrochloride (34 mg, 0.15 mmol) and AcOH (50 μL). The mixture was refluxed for 2 h. The reaction mixture was allowed to cool to room temperature and filtered. Then the precipitate was collected, washed with H$_2$O, and dried to afford **24a** (40 mg, 63%) as a red solid. Mp 259−261 °C. ^{1}H NMR (400 MHz, DMSO-d_6) δ: 1.93 (t, J = 8.0 Hz, 2H), 2.73 (t, J = 7.6 Hz, 2H), 3.40−3.44 (m, 2H), 7.20−7.39 (m, 7H), 7.70 (t, 1H), 7.75 (d, J = 8.4 Hz, 2H), 7.88 (t, J = 8.0 Hz, 1H), 8.11 (t, J = 8.0 Hz, 2H), 8.24 (d, J = 10.8 Hz, 2H), 9.01 (t, J = 5.2 Hz, 1H), 11.81 (s, 1H). ESI-MS m/z 488.2 [M + H]$^+$. HRMS (ESI) m/z calcd for $C_{26}H_{25}N_5O_3S$ [M + H]$^+$ 488.1756, found 488.1743.

2-((2-(4-(Aminosulfonyl)phenyl)hydrazinylidene)methyl)-N-(4-phenylbutyl)quinoline-4-carboxamide (24b). In the same manner as that described for the preparation of **24a**, **24b** was prepared from **21b** and 4-sulfonamidophenylhydrazine hydrochloride. Yield: 76%. Mp 251−254 °C. ^{1}H NMR (400 MHz, DMSO-d_6) δ: 1.63−1.73 (m, 4H), 2.67 (t, J = 6.8 Hz, 2H), 3.41−3.45 (m, 2H), 7.02 (d, J = 8.4 Hz, 1H), 7.18−7.31 (m, 6H), 7.38 (d, J = 8.4 Hz, 1H),

7.66−7.77 (m, 3H), 7.89 (t, J = 7.6 Hz, 1H), 8.06 (d, J = 7.6 Hz, 1H), 8.15 (d, J = 8.4 Hz, 1H), 8.21 (s, 1H), 8.27 (s, 1H), 9.00 (t, J = 8.8 Hz, 1H), 10.39 (br, 1H), 11.92 (br, 1H). ESI-MS m/z 502.3 [M + H]$^+$. HRMS (ESI) m/z calcd for $C_{27}H_{27}N_5O_3S$ [M + H]$^+$ 502.1913, found 502.1894.

2-((2-(3-Bromophenyl)hydrazinylidene)methyl)-N-(3-phenylpropyl)quinoline-4-carboxamide (24c). In the same manner as that described for the preparation of **24a**, **24c** was prepared from **21a** and 3-bromophenylhydrazine hydrochloride. Yield: 79%. mp 237−240 °C. ^{1}H NMR (400 MHz, DMSO-d_6) δ: 1.93 (t, J = 7.6 Hz, 2H), 2.72 (t, J = 8.0 Hz, 2H), 3.40−3.45 (m, 2H), 7.11 (d, J = 7.2 Hz, 1H), 7.19−7.33 (m, 7H), 7.54 (s, 1H), 7.74 (t, J = 7.6 Hz, 1H), 7.94 (t, J = 7.6 Hz, 1H), 8.14 (d, J = 8.0 Hz, 1H), 8.20 (d, J = 8.0 Hz, 1H), 8.31 (s, 2H), 9.10 (t, J = 5.2 Hz, 1H), 12.10 (s, 1H). ESI-MS m/z 487.2 [M + H]$^+$. HRMS (EI) m/z calcd for $C_{26}H_{23}BrN_4O$ (M$^+$) 486.1055, found 486.1036.

2-((2-(3-Bromophenyl)hydrazinylidene)methyl)-N-(4-phenylbutyl)quinoline-4-carboxamide (24d). In the same manner as that described for the preparation of **24a**, **24d** was prepared from **21b** and 3-bromophenylhydrazine hydrochloride. Yield: 60%. Mp 249−252 °C. ^{1}H NMR (400 MHz, DMSO-d_6) δ: 1.63−1.70 (m, 4H), 2.67 (t, J = 7.6 Hz, 2H), 3.42−3.44 (m, 2H), 7.17−7.28 (m, 8H), 7.54 (s, 1H), 7.72 (t, J = 8.0 Hz, 1H), 7.94 (t, J = 7.6 Hz, 1H), 8.10 (d, J = 8.0 Hz, 1H), 8.19 (d, J = 8.4 Hz, 1H), 8.28 (s, 2H), 9.07 (br, 1H), 12.09 (br, 1H). ESI-MS m/z 501.3 [M + H]$^+$. HRMS (ESI) m/z calcd for $C_{27}H_{25}BrN_4O$ [M + H]$^+$ 501.1290, found 501.1276.

2-((2-(3-Chlorophenyl)hydrazinylidene)methyl)-N-(3-phenylpropyl)quinoline-4-carboxamide (24e). In the same manner as that described for the preparation of **24a**, **24e** was prepared from **21a** and 3-chlorophenylhydrazine hydrochloride. Yield: 71%. Mp 253−255 °C. ^{1}H NMR (400 MHz, DMSO-d_6) δ: 1.91 (m, 2H), 2.73 (t, J = 8.0 Hz, 2H), 3.40−3.45 (m, 2H), 6.97 (d, J = 8.0 Hz, 1H), 7.20−7.35 (m, 7H), 7.40 (s, 1H), 7.73 (t, J = 7.6 Hz, 1H), 7.92 (t, J = 7.6 Hz, 1H), 8.13 (d, J = 8.0 Hz, 1H), 8.18 (d, J = 8.0 Hz, 1H), 8.29 (d, J = 8.0 Hz, 2H), 9.08 (br, 1H), 11.98 (s, 1H). ESI-MS m/z 443.2 [M + H]$^+$. HRMS (ESI) m/z calcd for $C_{26}H_{23}ClN_4O$ [M + H]$^+$ 443.1639, found 443.1624.

2-((2-(3-Chlorophenyl)hydrazinylidene)methyl)-N-(4-phenylbutyl)quinoline-4-carboxamide (24f). In the same manner as that described for the preparation of **24a**, **24f** was prepared from **21b** and 3-chlorophenylhydrazine hydrochloride. Yield: 55%. Mp 225−226 °C. ^{1}H NMR (400 MHz, DMSO-d_6) δ: 1.64−1.71 (m, 4H), 2.67 (t, J = 7.6 Hz, 2H), 3.41−3.46 (m, 2H), 7.01 (d, J = 7.6 Hz, 1H), 7.15−7.36 (m, 7H), 7.44 (s, 1H), 7.74 (t, J = 8.0 Hz, 1H), 7.97 (t, J = 8.0 Hz, 1H), 8.10 (d, J = 8.0 Hz, 1H), 8.24 (d, J = 8.0 Hz, 1H), 8.34 (s, 1H), 8.37 (s, 1H), 9.11 (t, J = 5.2 Hz, 1H), 12.35 (s, 1H). ESI-MS m/z 457.3 [M + H]$^+$. HRMS (ESI) m/z calcd for $C_{27}H_{25}ClN_4O$ [M + H]$^+$ 457.1795, found 457.1782.

2-((2-(3-Carboxyphenyl)hydrazinylidene)methyl)-N-(3-phenylpropyl)quinoline-4-carboxamide (24g). In the same manner as that described for the preparation of **24a**, **24g** was prepared from **21a** and 3-hydrazinobenzoic acid. Yield: 57%. Mp 259−262 °C. ^{1}H NMR (400 MHz, DMSO-d_6) δ: 1.92 (t, J = 7.6 Hz, 2H), 2.72 (t, J = 7.6 Hz, 2H), 3.38−3.43 (m, 2H), 7.21−7.50 (m, 8H), 7.62 (t, J = 7.2 Hz, 1H), 7.72 (s, 1H), 7.79 (t, J = 7.6 Hz, 1H), 8.01−8.09 (m, 4H), 8.95 (t, J = 5.2 Hz, 1H), 11.18 (s, 1H). ESI-MS m/z 453.2 [M + H]$^+$. HRMS (ESI) m/z calcd for $C_{27}H_{24}N_4O_3$ [M + H]$^+$ 453.1927, found 453.1912.

2-((2-(3-Carboxyphenyl)hydrazinylidene)methyl)-N-(4-phenylbutyl)quinoline-4-carboxamide (24h). In the same manner as that described for the preparation of **24a**, **24h** was prepared from **21b** and 3-hydrazinobenzoic acid. Yield: 88%. Mp 277 °C. ^{1}H NMR (400 MHz, DMSO-d_6) δ: 1.62−1.71 (m, 4H), 2.67 (t, J = 7.6 Hz, 2H), 3.42−3.44 (m, 2H), 7.11−7.28 (m, 8H), 7.54 (s, 1H), 7.72 (t, J = 7.6 Hz, 1H), 7.94 (t, J = 7.6 Hz, 1H), 8.09 (d, J = 8.0 Hz, 1H), 8.19 (d, J = 8.0 Hz, 1H), 8.28 (s, 2H), 9.07 (t, J = 5.2 Hz, 1H), 12.09 (s, 1H). ESI-MS m/z 467.4 [M + H]$^+$. HRMS (ESI) m/z calcd for $C_{28}H_{26}N_4O_3$ [M + H]$^+$ 467.2083, found 467.2067.

ASSOCIATED CONTENT

⊙ Supporting Information

General information for chemical agents and analytical measurements; detailed synthetic procedures and related spectroscopic data for starting materials of compounds **1** and **22l−n**; HPLC reports for the purity check of the compounds **1**, **22a−n**, **23a−m**, and **24a−h**; and the materials and methods of the reversed-phase HPLC analysis of protease inhibition assay. This material is available free of charge via the Internet at http://pubs.acs.org.

AUTHOR INFORMATION

Corresponding Author

*For W.T.: phone, +86-21-50806701; e-mail, tangwei@mail.shcnc.ac.cn. For C.-G.Y.: phone, +86-21-50806029; e-mail, yangcg@mail.shcnc.ac.cn. For J.L.: phone, +86-21-64252584; e-mail, jianli@ecust.edu.cn. For W.Z.: phone, +86-21-50805020; e-mail, wlzhu@mail.shcnc.ac.cn.

Author Contributions

$^\perp$These authors contributed equally to this work.

Notes

The authors declare no competing financial interest.

ACKNOWLEDGMENTS

ABBREVIATIONS USED

DENV, dengue virus; NS, nonstructural; SI, selectivity index; WNV, West Nile virus; YFV, yellow fever virus; JEV, Japanese encephalitis virus; DF, dengue fever; DHF, dengue hemorrhagic fever; DSS, dengue shock syndrome; IC$_{50}$, half-maximal inhibitory concentration; EC$_{50}$, half-maximal effective concentration; SAR, structure−activity relationship; EDCI, 1-(3-dimethylaminopropyl)-3-ethylcarbodiimide hydrochloride; CHAPS, 3-((3-cholamidopropyl)dimethylammonium)-1-propanesulfonate; DMSO, dimethylsulfoxide; PCR, polymerase chain reaction; BHK, baby hamster kidney; DMEM, Dulbecco's modified Eagle medium; FBS, fetal bovine serum; MTT, 3-(4,5-dimethylthiazol-2-yl)-2,5-diphenyltetrazolium bromide; CC$_{50}$, half-maximal cytotoxicity concentration; DCM, dichloromethane; DMF, N,N-dimethylformamide

REFERENCES

(1) Stevens, A. J.; Gahan, M. E.; Mahalingam, S.; Keller, P. A. The medicinal chemistry of dengue fever. *J. Med. Chem.* **2009**, *52*, 7911−7926.

(2) Chua, J. E.; Ng, M. L.; Chow, T. K. The non-structural 3 (NS3) protein of dengue virus type 2 interacts with human nuclear receptor binding protein and is associated with alterations in membrane structure. *Virus Res.* **2004**, *102*, 151−163.

(3) Marks, R. M.; Lu, H.; Sundaresan, R.; Toida, T.; Suzuki, A.; Imanari, T.; Hernáiz, M. J.; Linhardt, R. J. Probing the interaction of dengue virus envelope protein with heparin: assessment of

glycosaminoglycan-derived inhibitors. *J. Med. Chem.* **2001**, *44*, 2178−2187.

(4) Morens, D. M.; Fauci, A. S. Dengue and hemorrhagic fever: a potential threat to public health in the United States. *JAMA, J. Am. Med. Assoc.* **2008**, *299*, 214−216.

(5) Dengue and Severe Dengue. http://www.who.int/mediacentre/factsheets/fs117/en/ (accessed June 9, 2011).

(6) Yin, Z.; Chen, Y. L.; Kondreddi, R. R.; Chan, W. L.; Wang, G.; Ng, R. H.; Lim, Y. H.; Lee, W. Y.; Jeyaraj, D. A.; Niyomrattanakit, P.; Wen, D.; Chao, A.; Glickman, J. F.; Voshol, H.; Mueller, D.; Spanka, C.; Dressler, S.; Nilar, S.; Vasudevan, S. G.; Shi, P. Y.; Keller, T. H. *N*-Sulfonylanthranilic acid derivatives as allosteric inhibitors of dengue viral RNA-dependent RNA polymerase. *J. Med. Chem.* **2009**, *52*, 7934−7937.

(7) Nair, V.; Chi, G.; Shu, Q.; Julander, J.; Smee, D. F. A heterocyclic molecule with significant activity against dengue virus. *Bioorg. Med. Chem. Lett.* **2009**, *19*, 1425−1427.

(8) Rice, C. M.; Lenches, E. M.; Eddy, S. R.; Shin, S. J.; Sheets, R. L.; Strauss, J. H. Nucleotide sequence of yellow fever virus: implications for flavivirus gene expression and evolution. *Science* **1985**, *229*, 726−733.

(9) Chambers, T. J.; Hahn, C. S.; Galler, R.; Rice, C. M. Flavivirus genome organization, expression, and replication. *Annu. Rev. Microbiol.* **1990**, *44*, 649−688.

(10) Bazan, J. F.; Fletterick, R. J. Detection of a trypsin-like serine protease domain in flaviviruses and pestiviruses. *Virology* **1989**, *171*, 637−639.

(11) Sampatha, A.; Padmanabhan, R. Molecular targets for flavivirus drug discovery. *Antiviral Res.* **2009**, *81*, 6−15.

(12) Gorbalenya, A. E.; Donchenko, A. P.; Koonin, E. V.; Blinov, V. M. N-Terminal domains of putative helicases of flavi- and pestiviruses may be serine proteases. *Nucleic Acids Res.* **1989**, *17*, 3889−3897.

(13) Yusof, R.; Clum, S.; Wetzel, M; Murthy, H. M.; Padmanabhan, R. Purified NS2B/NS3 serine protease of dengue virus type 2 exhibits cofactor NS2B dependence for cleavage of substrates with dibasic amino acids in vitro. *J. Biol. Chem.* **2000**, *275*, 9963−9969.

(14) Zuo, Z.; Liew, O. W.; Chen, G.; Chong, P. C. J.; Lee, S. H.; Chen, K.; Jiang, H.; Puah, C. M.; Zhu, W. Mechanism of NS2B-mediated activation of NS3pro in dengue virus: molecular dynamics simulations and bioassays. *J. Virol.* **2009**, *83*, 1060−1070.

(15) Falgout, B.; Pethel, M.; Zhang, Y. M.; Lai, C. J. Both nonstructural proteins NS2B and NS3 are required for the proteolytic processing of dengue virus nonstructural proteins. *J. Virol.* **1991**, *65*, 2467−2475.

(16) Valle, R. P.; Falgout, B. Mutagenesis of the NS3 protease of dengue virus type 2. *J. Virol.* **1998**, *72*, 624−632.

(17) Lescar, J; Luo, D.; Xu, T.; Sampath, A.; Lim, S. P.; Canard, B.; Vasudevan, S. G. Towards the design of antiviral inhibitors against flaviviruses: the case for the multifunctional NS3 protein from dengue virus as a target. *Antiviral Res.* **2008**, *80*, 94−101.

(18) Noble, C. G.; Chen, Y. L.; Dong, H. P.; Gu, F.; Lim, S. P.; Schul, W.; Wang, Q. Y.; Shi, P. Y. Strategies for development of dengue virus inhibitors. *Antiviral Res.* **2010**, *85*, 450−462.

(19) Yin, Z.; Patel, S. J.; Wang, W. L.; Chan, W. L.; Rao, K. R.; Wang, G.; Ngew, X. Y.; Patel, V.; Beer, D.; Knox, J. E.; Ma, N. L.; Ehrhardt, C.; Lim, S. P.; Vasudevana, S. G.; Keller, T. H. Peptide inhibitors of dengue virus NS3 protease. Part 2: SAR study of tetrapeptide aldehyde inhibitors. *Bioorg. Med. Chem. Lett.* **2006**, *16*, 40−43.

(20) Yin, Z.; Patel, S. J.; Wang, W. L.; Wang, G.; Chan, W. L.; Rao, K. R.; Alam, J.; Jeyaraj, D. A.; Ngew, X. Y.; Patel, V.; Beer, D.; Lim, S. P.; Vasudevan, S. G.; Keller, T. H. Peptide inhibitors of dengue virus NS3 protease. Part 1: Warhead. *Bioorg. Med. Chem. Lett.* **2006**, *16*, 36−39.

(21) Chanprapaph, S.; Saparpakorn, P.; Sangma, C.; Niyomrattanakit, P.; Hannongbua, S.; Angsuthanasombat, C.; Katzenmeier, G. Competitive inhibition of the dengue virus NS3 serine protease by synthetic peptides representing polyprotein cleavage sites. *Biochem. Biophys. Res. Commun.* **2005**, *330*, 1237−1246.

(22) Gao, Y.; Cui, T.; Lam, Y. Synthesis and disulfide bond connectivity−activity studies of a kalata B1-inspired cyclopeptide

against dengue NS2B-NS3 protease. *Bioorg. Med. Chem.* **2010**, *18*, 1331−1336.

(23) Tomlinson, S. M.; Malmstrom, R. D.; Russo, A.; Mueller, N.; Pang, Y. P.; Watowich, S. J. Structure-based discovery of dengue virus protease inhibitors. *Antiviral Res.* **2009**, *82*, 110−114.

(24) Tomlinson, S. M.; Watowich, S. J. Anthracene-based inhibitors of dengue virus NS2B-NS3 protease. *Antiviral Res.* **2011**, *89*, 127−135.

(25) Knehans, T.; Schüller, A.; Doan, D. N.; Nacro, K.; Hill, J.; Güntert, P.; Madhusudhan, M. S.; Weil, T.; Vasudevan, S. G. Structure-guided fragment-based in silico drug design of dengue protease inhibitors. *J. Comput.-Aided. Mol. Des.* **2011**, *25*, 263−274.

(26) Kiat, T. S.; Pippen, R.; Yusof, R.; Ibrahim, H.; Khalid, N.; Rahman, N. A. Inhibitory activity of cyclohexenyl chalcone derivatives and flavonoids of fingerroot, *Boesenbergia rotunda* (L.), towards dengue-2 virus NS3 protease. *Bioorg. Med. Chem. Lett.* **2006**, *16*, 3337−3340.

(27) Hidari, K. I.; Takahashi, N.; Arihara, M.; Nagaoka, M.; Morita, K.; Suzuki, T. Structure and anti-dengue virus activity of sulfated polysaccharide from a marine alga. *Biochem. Biophys. Res. Commun.* **2008**, *376*, 91−95.

(28) Frimayanti, N.; Chee, C.; Zain, S. M.; Rahman, N. A. Design of new competitive dengue Ns2b/Ns3 protease inhibitors—a computational approach. *Int. J. Mol. Sci* **2011**, *12*, 1089−1100.

(29) Yang, C. C.; Hsieh, Y. C.; Lee, S. J.; Wu, S. H.; Liao, C. L.; Tsao, C. H.; Chao, Y. S.; Chern, J. H.; Wu, C. P.; Yueh, A. Novel dengue virus-specific NS2B/NS3 protease inhibitor, BP2109, discovered by a high-throughput screening assay. *Antimicrob. Agents Chemother.* **2011**, *55*, 229−238.

(30) Steuer, C.; Gege, C.; Fischl, W.; Heinonen, K. H.; Bartenschlagerb, R.; Klein, C. D. Synthesis and biological evaluation of alpha-ketoamides as inhibitors of the dengue virus protease with antiviral activity in cell-culture. *Bioorg. Med. Chem.* **2011**, *19*, 4067−4074.

(31) Erbel, P.; Schiering, N.; D'Arcy, A.; Renatus, M.; Kroemer, M.; Lim, S. P.; Yin, Z.; Keller, T. H.; Vasudevan, S. G.; Hommel, U. Structural basis for the activation of flaviviral NS3 proteases from dengue and West Nile virus. *Nat. Struct. Mol. Biol.* **2006**, *13*, 372−373.

(32) Ewing, T.; Kuntz, I. D. Critical evaluation of search algorithms for automated molecular docking and database screening. *J. Comput. Chem.* **1997**, *18*, 1175−1189.

(33) Kuntz, I. D. Structure-based strategies for drug design and discovery. *Science* **1992**, *257*, 1078−1082.

(34) Eldridge, M. D.; Murray, C. W.; Auton, T. R.; Paolini, G. V.; Mee, R. P. Empirical scoring functions: I. the development of a fast empirical scoring function to estimate the binding affinity of ligands in receptor complexes. *J. Comput.-Aided Mol. Des.* **1997**, *11*, 425−445.

(35) *Sybyl* (Molecular Modeling Package), version 6.8; Tripos Associates: St. Louis, MO, 2000.

(36) Lauri, G.; Bartlett, P. A. CAVEAT: a program to facilitate the design of organic molecules. *J. Comput.-Aided Mol. Des.* **1994**, *8*, 51−66.

(37) Leung, D.; Schroder, K.; White, H.; Fang, N. X.; Stoermer, M. J.; Abbenante, G.; Martin, J. L.; Young, P. R.; Fairlie, D. P. Activity of recombinant dengue 2 virus NS3 protease in the presence of a truncated NS2B co-factor, small peptide substrates, and inhibitors. *J. Biol. Chem.* **2001**, *276*, 45762−45771.

(38) Steuer, C.; Heinonen, K. H.; Kattner, L.; Klein, C. D. Optimization of assay conditions for dengue virus protease: effect of various polyols and nonionic detergents. *J. Biomol. Screening* **2009**, *14*, 1102−1108.

(39) Khumthong, R.; Angsuthanasombat, C.; Panyim, S.; Katzenmeier, G. In vitro determination of dengue virus type 2 NS2B-NS3 protease activity with fluorescent peptide substrates. *J. Biochem. Mol. Biol.* **2002**, *35*, 206−212.